This article was downloaded by:
On: *21 January 2011*
Access details: *Access Details: Free Access*
Publisher *Taylor & Francis*
Informa Ltd Registered in England and Wales Registered Number: 1072954 Registered office: Mortimer House, 37-41 Mortimer Street, London W1T 3JH, UK

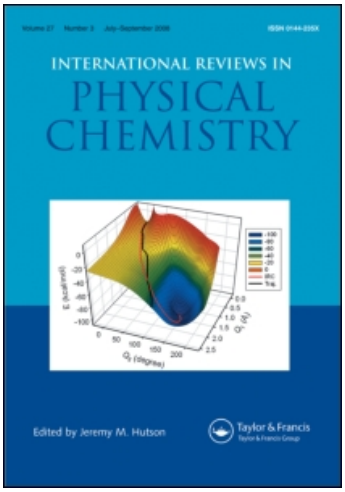

International Reviews in Physical Chemistry
Publication details, including instructions for authors and subscription information:
http://www.informaworld.com/smpp/title~content=t713724383

Underpotential deposition of metals on foreign metal substrates

S. Szabó[a]
[a] Central Research Institute of Chemistry, Hungarian Academy of Sciences, Hungary

To cite this Article Szabó, S.(1991) 'Underpotential deposition of metals on foreign metal substrates', International Reviews in Physical Chemistry, 10: 2, 207 — 248
To link to this Article: DOI: 10.1080/01442359109353258
URL: http://dx.doi.org/10.1080/01442359109353258

PLEASE SCROLL DOWN FOR ARTICLE

Full terms and conditions of use: http://www.informaworld.com/terms-and-conditions-of-access.pdf

This article may be used for research, teaching and private study purposes. Any substantial or systematic reproduction, re-distribution, re-selling, loan or sub-licensing, systematic supply or distribution in any form to anyone is expressly forbidden.

The publisher does not give any warranty express or implied or make any representation that the contents will be complete or accurate or up to date. The accuracy of any instructions, formulae and drug doses should be independently verified with primary sources. The publisher shall not be liable for any loss, actions, claims, proceedings, demand or costs or damages whatsoever or howsoever caused arising directly or indirectly in connection with or arising out of the use of this material.

INTERNATIONAL REVIEWS IN PHYSICAL CHEMISTRY, 1991, VOL. 10, NO. 2, 207–248

Underpotential deposition of metals on foreign metal substrates

by S. SZABÓ
Central Research Institute of Chemistry, Hungarian Academy of Sciences,
H-1525 Budapest, P.O. Box 17, Hungary

The underpotential deposition of metals on foreign metal substrates has been reviewed, but this term is used in a wider sense in this monograph. All the redox processes resulting in adsorbed metal atoms on foreign metal substrates are included in this term. Based on the source of electrons taking part in the underpotential deposition, the classification of the processes leading to adsorbed metal atoms is also given.

Downloaded At: 17:40 21 January 2011

1. Introduction

The anomalous behaviour of small amounts of metals electrodeposited on foreign metal substrates has been known for a very long time [1, 2]. The anomaly is the apparent violation of Nernst's law, that is, a part of the metals electrodeposited on foreign metal surfaces is oxidized at a much more positive potential than the reversible Nernst potential in the same electrolyte. Later, the potential difference between the oxidation potential of submonolayer amounts of metals deposited on 'inert' foreign metal substrates and the reversible Nernst potential of the depositing metal in the same electrolyte was called underpotential shift and the process itself underpotential deposition (UPD). (It must be taken into consideration that this phenomenon has also been termed metal adsorption [3], adatom deposition [4], chemisorption of metals [5], electrosorption of metals or metal ions [6, 7], specific adsorption or adsorption of cations [8, 9], formation of monolayer metal films [10], ...)

The adsorption of metals on foreign metal substrates has been studied also in gaseous phase in ultra-high vacuum [11]. Investigations in this field started only in the mid-1930s. The two fields developed separately, without any interrelation between the two areas. A few papers have been published recently in which electrochemical and surface chemical methods were applied simultaneously [12, 13].

This strong separation of the two fields can be explained by the different experimental techniques rendering difficult communication between the two fields.

There are other reasons for this strong isolation. In the course of underpotential deposition, besides metal adsorption a charge-transfer process must also take place. Therefore underpotential deposition is sometimes called electrochemical metal adsorption to distinguish this process from vapour-phase metal adsorption [14].

In contrast to metal adsorption from the gas phase, electrosorption of metals on foreign metal substrates depends on the potential of the substrate metal. In addition, adsorption takes place under the influence of the double layer, which renders adsorption even more complicated.

Because of the charge-transfer processes, underpotential deposition is regarded mostly as an electrochemical phenomenon in electrochemistry, sometimes ignoring the non-electrochemical aspects of metal adsorption or the possibility of such redox processes resulting also in adsorbed metal layers on foreign metal surfaces without electrochemical manipulation.

0144–235X/91 $3·00 © 1991 Taylor & Francis Ltd.

For the above reasons, in this article the term underpotential deposition (UPD) will be used in a wider sense. All the redox processes resulting in adsorbed metal atoms on foreign metal surfaces are included in this term.

Based on the source of electrons taking part in the deposition of adsorbed metal atoms on foreign metal surfaces, the redox processes resulting in adsorbed metal layers can be classified. The classification is also included in this article.

2. General description of the phenomenon

Underpotential deposition (UPD) of metals is an electroreduction of metallic ions on foreign metal substrates (S) in the so-called underpotential range (ΔU), that is, in a potential region positive to the Nernst potential (E_N) of the depositing M^{z+}/M couple [10, 15–18]:

$$\Delta U = E_{ads} - E_N \geqslant 0. \tag{1}$$

The reason for the underpotential deposition is the excess binding energy of an adsorbed metal atom on a foreign metal surface ($S–M_{ads}$) relative to the binding energy of a deposited metal atom on a surface of its own kind ($M–M_{ads}$):

$$S–M_{ads} \geqslant M–M_{ads}. \tag{2}$$

The binding energy is independent of the equilibrium at the metal–electrolyte interface, and consequently of the electrode potential at which the deposition took place [19, 20].

Therefore, in practice, all deposited metals oxidized at a more positive potential (E_{ads}) than the Nernst potential of the depositing ion are taken for an underpotentially deposited metal irrespective of whether electroreduction (or reduction by any reducing agent) was carried out in underpotential or in overpotential region.

UPD (ΔU), which is sometimes called underpotential shift [19], extends from a few millivolts to over several hundred millivolts, depending on the strength of adsorbate substrate interactions, namely on the system studied.

The ΔU values depend on the crystal faces on which metal adsorption takes place and thus the underpotential deposition of metals on foreign metal surfaces has a multiple-state character [4, 16, 21].

Sometimes irreversible adsorption [22, 23] and even alloy formation can be observed [24, 25].

Underpotential deposition can easily be observed as waves on constant current charging curves [5, 22, 26] or as current peaks on potentiodynamic curves [4, 15]. The values of the underpotential (ΔU) are usually measured at the waves and peaks of polarization curves [15].

3. The thermodynamics of underpotential deposition

In the course of underpotential deposition of metals on foreign metal surfaces (S) the ions of the depositing metal (M^{z+}) penetrate into the double layer and come in direct contact with the substrate metal (S) [26, 27, 28]. During this process adsorbed water molecules are removed from the surface of the substrate metal and the solvation shell of the depositing ions will be partly or completely destroyed [27]. Depending on the chemical nature of the interaction between adsorbent (S) and adsorbate (M^{z+}) a purely physical bond or a much stronger chemical bond is formed. If a chemical bond (chemisorption) is formed (which can only be considered as underpotential deposition) then partial charge transfer of λ electrons will take place from the substrate metal to the depositing ions [26–28] (figure 1).

Downloaded At: 17:40 21 January 2011

Underpotential deposition can be described by the following electrochemical reaction [26–28]:

$$\nu S\text{–}OH_2 + M^{z+}.aq + \lambda e \rightleftharpoons S_\nu\text{–}M_{ads}^{(z-\lambda)+} + \nu H_2O.aq, \tag{3}$$

λ is the partial charge transfer coefficient, introduced by Lorenz and Salié [29]. λ takes into account the fact that the transfer of charge goes on in non-integral elementary steps during an electrosorption reaction. The charge transfer coefficient is defined by the difference between the actual charge of the deposited metal atom (z_{ads}) and the ionic charge of the adsorbing ions (z):

$$\lambda = z - z_{ads}. \tag{4}$$

The partial charge on adsorbed metal atoms is usually small and cannot be determined experimentally [26–29].

In a few papers [18, 30, 31] the partial charge transfer coefficient is substituted for electrosorption valency (γ). When γ is used in place of λ then the change of potential of zero charge and double layer structure due to underpotential deposition is ignored.

From the concept of partial charge transfer it follows that the adsorbing metal ions penetrate into the double layer and they are held at a certain potential (potential of adsorption φ_{ads}) which is smaller than the potential of the substrate (φ_S). Therefore the adsorbed species are affected by only a fraction of the total potential drop across the compact double layer (Helmholtz layer):

$$\varphi_{ads} \lesseqgtr \varphi_S. \tag{5}$$

The position of the adsorbed ions in the Helmholtz layer is described by a geometric factor (g) [16, 27, 28, 32, 33]:

$$g = (\varphi_{ads} - \varphi_e)/(\varphi_S - \varphi_e), \tag{6}$$

where φ_e is the potential of the adsorbing ions in the supporting electrolyte. In the case of underpotential deposition without supporting electrolyte it must be taken into account that $\varphi_h - \varphi_e \neq 0$, (where φ_h is the potential in the Helmholtz layer) and φ_e has to be substituted for φ_h in equation (6) [27, 28, 32, 33].

3.1. *The potential dependence of electrosorption equilibrium*

3.1.1. *Quasi-Nernstian formalism*

If ionic charge on the adsorbed metal atoms is low ($z_{ads} \approx 0$), indicating the absence of coadsorption phenomena, then the sorption behaviour of M^{z+} can be described by a quasi-Nernst equation [10, 17, 32]:

$$E = E_o + \frac{RT}{zF} \ln \frac{a_{M^{z+}}}{a(\Gamma)}, \tag{7}$$

where the activity of the M_{ads}adsorbate ($a(\Gamma)$) represents the system specific type of isotherm as a function of Γ only [17].

3.1.2. *Electrosorption valency* (γ)

The potential dependence of electrosorption equilibrium and the charge flow of electrosorption processes during the electrosorption reaction can be described by

Downloaded At: 17:40 21 January 2011

electrosorption valency (γ) [27, 28, 32–34]. In the case of excess supporting electrolyte (when $\varphi_h = \varphi_e$) the electrosorption valency is defined by equation (8) [27, 28, 32–34]:

$$\gamma F = -\left(\frac{\partial q_S}{\partial \Gamma}\right)_E = \left(\frac{\partial \mu_M}{\partial E}\right)_{\Gamma_{ads}}, \tag{8}$$

where μ_M is the chemical potential of M^{z+} in the supporting electrolyte, E is the electrode potential, q_S is the substrate charge and Γ_{ads} is the surface concentration of the adsorbed metal. Equation (8) can be used at either ideally polarizable or at reversible electrodes remembering that in the absence of excess supporting electrolyte μ_M must be replaced by the chemical potential of the depositing ions in the Helmholtz layer (μ_{Mh}) and E must be substituted by the potential drop across compact double layer ($\Delta\varphi$) [27].

Another restriction, is that in this form equation (8) cannot be applied to mixed electrosorption systems [34–36]. The thermodynamic treatment of the problem yielded an equation similar to equation (8) but with a 'mixed electrosorption valency' [34, 36]. In the case of a second electrosorbed substance, X, the γ_{mix} is the sum of the two single valencies

$$\gamma_{mix} = \gamma + \rho\gamma_X, \tag{9}$$

where ρ is the coupling factor ($\rho = \partial\Gamma_{X,ads}/\partial\Gamma_{Mads})_{E,\mu_X}$) which is positive in co-adsorption and negative in competitive electrosorption [36].

Electrosorption valency is equivalent to the Nernst valency and controls potential dependence and charge flow during underpotential deposition in the same way as z does in the case of electrodeposition of metals [27, 34].

Downloaded At: 17:40 21 January 2011

3.1.2.1. *Interpretation of electrosorption valency*

In contrast to the Nernst or Faraday valency, electrosorption valency can be a fractional number dependent on different variables. Comprehensive treatment of electrosorption reactions resulted in relations in which electrosorption valency is correlated with non-measurable microscopic features of the system [27, 28, 32–34].

Electrosorption valency at the potential of zero charge (E_{PZC}) is given by equation (10) [27, 28, 32]

$$\gamma_{PZC} = gz - \lambda(1-g) + k_M - \nu k_w, \tag{10}$$

where k_M and k_w are dipole terms of adsorbed metal (k_M) and desorbed water (k_w) which take into account that part of the electrical energy which is due to oriented dipoles with dipole moment m_i [27, 28]:

$$k_i = \pm\frac{m_i}{e_o l_i} \tag{11}$$

where m_i/e_o is the dipole length and

$$l_i = \frac{\varphi_S - \varphi_E}{dE/dx}, \tag{12}$$

provided the use of excess supporting electrolyte. ν is the number of solvent molecules displaced by one adsorbed atom.

For metal adatoms $\nu = 0$ if it is assumed that the water molecules displaced by adsorbed atoms will adsorb again on adatoms in the same way as on the substrate [16].

In the case of underpotential deposition of metals k_M is also zero, hence the electrosorption valency at the potential of zero charge is [28]

$$\gamma_{PZC} \approx gz - \lambda(1-g). \tag{13}$$

At potentials distinct from the potential of zero charge the electrosorption valency can only be calculated if its dependence on the potential is taken into consideration. According to thermodynamic analysis the potential dependence is brought about by the change in the double layer capacity (C_D) due to increasing surface concentration of adsorbed material (Γ_{ads}) [27, 28, 32, 33]:

$$\gamma = \gamma_{PZC} - \frac{1}{F} \int_{E_{PZC}}^{E} \left(\frac{\partial C_D}{\partial \Gamma} \right)_E \mathrm{d}E, \tag{14}$$

where $C_D = (\partial q_S / \partial E)_{\Gamma_{ads}}$ when excess supporting electrolyte is used. Electrosorption valencies for cationic systems in aqueous solutions at small coverages hardly depend on potential ($\mathrm{d}\gamma/\mathrm{d}E \approx 0$) and thus $\gamma \approx \gamma_{PZC}$ [28].

Although occasionally electrosorption valencies of cationic systems depend strongly on coverages (UPD of Cu^{2+} ions on Pt [26]) there are systems where such dependence cannot be observed (UPD of H^+ ions on Pt [27]).

The effect of temperature on electrosorption valency seems to be negligible because g and λ are expected to be temperature independent [28].

3.1.2.2. *Determination of electrosorption valency*

(*a*) Determination from charge flow

If the surface concentration of adsorbed metal can be measured then on the basis of equation (8) the electrosorption valency can be calculated. As follows from this equation, the substrate metal charge, q_S, must be measured or calculated at constant E [27, 28].

(*b*) Determination from potential dependence

If activity coefficients are constant, μ_M in equation (8) can be substituted by the concentration of the depositing ions c_M. At constant coverage of the deposited metal atoms the derivative $(\partial \ln c_M / \partial E)_{\Gamma_{ads}}$ yields γ [27, 28].

(*c*) Determination from kinetic measurements

Electrosorption valency can be determined from the sum of electrochemical transfer coefficients $\alpha + \beta$ [27, 28]:

$$(\alpha + \beta) z = \gamma. \tag{15}$$

3.1.3. *Submonolayer equilibrium potential*

When the underpotential deposition of metals takes place with partial charge transfer then equation (7) cannot be used to describe the equilibrium between the depositing ions (M^{z+}) and adsorbed species (M_{ads}) because differences may occur between the value of electrosorption valency (γ) and the charge ($z+$) on the metal ions in the electrolyte and thus monolayer activity does not exhibit a simple exponential dependence on the electrode potential.

The description of equilibrium properties in this case is based on the concept of 'submonolayer equilibrium potential' (E_{ML}) which is developed on the basis of equal electrochemical potentials of the adsorbed species in solution and on the substrate surface, due to the charge transfer equilibrium of reaction (3) [18, 37, 38].

Downloaded At: 17:40 21 January 2011

The submonolayer equilibrium potential (E_{ML}) is defined as follows [18, 38]:

$$E_{ML} = E^{\circ}_{ML} + \frac{RT}{\gamma F} \ln\left(\frac{a_{M^{z+}}}{a_{ML}}\right), \tag{16}$$

where $a_{M^{z+}}$ is the activity of the depositing metal ion in the supporting electrolyte and a_{ML} is the activity of the adsorbed metal atoms at a coverage between 0 and 1. a_{ML} depends on the adsorption isotherm that can be applied to describe the activity of the adsorbed species and on the multiple energy states if these exist [18, 38]. E°_{ML} is the standard submonolayer potential and is connected with the standard free energy of the formation of a submonolayer [38]:

$$\Delta G^{\circ}_{ML} = \gamma F E^{\circ}_{ML}, \tag{17}$$

E°_{ML} and consequently ΔG°_{ML} depends on the adsorption isotherm that can be used to describe the activity of the adsorbed species in the same way as a_{ML} does.

By definition of the submonolayer equilibrium potential a more correct definition can be given for the underpotential (shift) by substituting E_{ads} for E_{ML} in equation (1) ($\Delta U = E_{ML} - E_N$) [18, 38].

The underpotential (ΔU) in an explicit form is

$$\Delta U = (E^{\circ}_{ML} - E^{\circ}) + \frac{RT}{F}\left(\frac{1}{\gamma} - \frac{1}{z}\right) \ln a_{M^{z+}} - \frac{RT}{\gamma F} \ln a_{ML}, \tag{18}$$

where

$$E^{\circ}_{ML} - E^{\circ} = \Delta U^{\circ} = \frac{\Delta G^{\circ}}{zF} - \frac{\Delta G^{\circ}_{ML}}{\gamma F}, \tag{19}$$

where E° is the standard equilibrium potential for the bulk M/M^{z+} couple and ΔG° its standard free-energy change [18, 38].

3.2. *Underpotential coverage isotherms*

Based on the concept of submonolayer equilibrium potential, underpotential-coverage (θ) isotherms can be derived relying upon equations (18) and (19). In the course of derivation, however, the dependence of monolayer free energy on coverage (θ) and the existence of multiple energy states in the monolayer range have to be taken into account [18, 38]. (Coverage (θ) means the coverage of adsorbed metal (M_{ads}) on substrate S if otherwise not stated.)

3.2.1. *No interaction case*

The hypothetical absence of interaction between the adsorbed species and the absence of their interaction with the substrate leads to a Langmuir-type adsorption. The Langmuir adsorption isotherm can generally be applied to electrosorption reactions when the coverage is below 0·2 [38].

If Langmuir-type adsorption exists, the adsorption isotherms of metals adsorbed on foreign metal surfaces for single energy state, can be derived from equation (18) since

$$a_{ML} = \frac{\theta}{1-\theta}. \tag{20}$$

By substitution of equation (20) into equation (18), the new equation can be used in potentiodynamic experiments if the desorption of UPD species is reversible. At $\theta = 0{\cdot}5$

Downloaded At: 17:40 21 January 2011

and at unit activity of the depositing ions in the supporting electrolyte the standard free energy (ΔG°_{ML}) of formation of adsorbed metal monolayer can be determined.

Under Langmuir conditions, the half-width of a monolayer stripping peak of a univalent adsorbed metal is about 0·09 V. Broadening of the stripping peak can very often be observed. This has been explained by the large lattice mis-match between the substrate and adsorbate and a 'dissociative' Langmuir isotherm has been suggested [39] to explain such results.

3.2.2. *Particle–substrate interactions*

The idealized model of the Langmuir adsorption isotherm can very often not be applied to characterize underpotential deposition since most substrate surfaces are energetically heterogeneous and thus the monolayer free energy depends on the coverage. Another important factor is the change in work function of the substrate as a consequence of the formation of an adsorbed metal monolayer [38].

If it is assumed that the monolayer free energy decreases linearly with coverage (the Temkin concept) [38]:

$$\Delta G^{\circ}_{ML} = \Delta G^{\theta\to 0}_{ML} + fRT\theta, \tag{21}$$

where $\Delta G^{\theta\to 0}$ is the free energy change of adsorption at the beginning of underpotential deposition. The underpotential (ΔU) can then be calculated in the case of particle–substrate interactions by substituting equation (21) into equation (18) taking into account equation (19) and thus

$$\Delta U = \left(\frac{\Delta G^{\circ}}{zF} - \frac{\Delta G^{\theta\to 0}_{ML}}{\gamma F}\right) + \frac{RT}{F}\left(\frac{1}{\gamma} - \frac{1}{z}\right)\ln a_{M^{z+}} - \frac{RT}{\gamma F}\left[\ln\left(\frac{\theta}{1-\theta}\right) + f\theta\right], \tag{22}$$

$\Delta G^{\theta\to 0}_{ML}$ can be obtained from the intercept of the ΔU against $f\theta + \ln[\theta/(1-\theta)]$ diagram. The value of the electrosorption valency must be determined in a separate experiment.

Usually very large Temkin parameters can be measured for adsorbed metal species. The high Temkin parameters cannot be explained wholly by particle–particle interaction.

Work function differences measured at the metal/gas interface verified that the Temkin parameter (f) is predominantly determined by particle substrate interactions during underpotential deposition [18]. The correlation between underpotential shifts and work-function differences indicates also the existence of particle–substrate interactions in UPD processes [15, 19].

3.2.3. *Particle–particle interactions*

In addition to particle–substrate interactions the contribution of lateral interaction energy to the variation of monolayer free energy can also be expected even without partially charged species in UPD layers [18]. In addition, the presence of partially discharged species in the adsorbed metal layer gives rise to repulsive forces [40]. An UPD layer composed of partially discharged ions has a tendency to attract oppositely charged ions [6, 7] so that the repulsive forces will be screened or even converted to attractive forces. This can be identified by its $\theta^{3/2}$ dependence [40].

The standard free energy of formation of a monolayer for these interactions is [18, 38]

$$\Delta G^{\circ}_{ML} = \Delta G^{\theta\to 0}_{ML} + fRT\theta + gRT\theta^{3/2}, \tag{23}$$

Downloaded At: 17:40 21 January 2011

where g is the interaction parameter defined in reference [40]. (In equation (23) g may be considered also to be a Frumkin parameter.) Thus the expression for underpotential in the presence of particle–substrate and particle–particle interactions is [38]

$$\Delta U = \left(\frac{\Delta G^{\circ}}{zF} - \frac{\Delta G_{ML}^{\theta\to 0}}{\gamma F}\right) + \frac{RT}{F}\left(\frac{1}{\gamma} - \frac{1}{z}\right)\ln a_{M^{z+}} - \frac{RT}{\gamma F}\left[\ln\left(\frac{\theta}{1-\theta}\right) + f\theta + g\theta^{3/2}\right], \quad (24)$$

where

$$\frac{\Delta G^{\circ}}{zF} - \frac{\Delta G_{ML}^{\theta\to 0}}{\gamma F} = \Delta U^{\theta\to 0}. \quad (25)$$

When electrosorption valency (γ) is hardly lower than the ionic charge ($z+$) of the depositing ions, that is $\gamma \approx z$, which is usually the case, then equation (24) can be simplified [18]:

$$\Delta U = \Delta U^{\theta\to 0} - \frac{RT}{\gamma F}\left[\ln\left(\frac{\theta}{1-\theta}\right) + f\theta + g\theta^{3/2}\right], \quad (26)$$

and then the dependence of ΔU on the activity of depositing ions in the supporting electrolyte vanishes [18].

Downloaded At: 17:40 21 January 2011

3.2.4. *General isotherm*

The adsorption isotherms defined above have a Langmuir basis, which implies the additivity of particle–particle and particle–substrate interactions. These isotherms can be applied to describe adsorption processes of underpotential deposition if the adsorbed monolayer constitutes of single energy state [18]. When metal monolayers formed by underpotential deposition are composed of multiple energy states and the various states do not interact with each other then each energy state can be described by an adsorption isotherm based on the Langmuir concept [18].

Assuming additivity of interactions, we may write the general isotherm for the jth state as follows [18]:

$$\Delta U = \Delta U_j^{\theta\to\theta_{j-1}} + \frac{RT}{F}\left(\frac{1}{\gamma} - \frac{1}{z}\right)\ln a_{M^{z+}} - \frac{RT}{\gamma F}\left[\ln\left(\frac{\theta-\theta_{j-1}}{\theta_j-\theta}\right) + f_j(\theta-\theta_{j-1}) + g_j(\theta-\theta_{j-1})^{3/2}\right], \quad (27)$$

where θ_{j-1} is the initial and θ_j is final coverage of the jth energy state. Equation (27) can be considered to be a general isotherm. When $\theta_{j-1}=0$ and $\theta_j=1$ then equation (27) becomes the general isotherm of an adsorbed monolayer with a single energy state.

3.2.5. *Interaction effects in electrodeposited monolayers*

The simplified model of $\theta^{3/2}$ dependence of particle–particle interactions (section 3.2.3) does not properly describe the interaction effects in monolayers formed by underpotential deposition. A more correct treatment can be given to the phenomenon based on the application of the concept of adsorption pseudo-capacitance [21, 30, 40].

This section will examine how partially charged adsorbed atoms should behave in a two-dimensional lattice in relation to the deviation of γ from z. Two effects arise in consequence of $\gamma < z$. Even in the hypothetical absence of coulombic repulsive effects, an important effect of $\gamma < z$ on the shape of the adsorption isotherm can be predicted

because a broader range of potential is required to achieve full coverage. In addition to this effect, the Coulombic interactions between the partially charged atoms will cause an additional change of energy of adsorption and widening of capacitance (C) against potential (E) profile [30, 40].

3.2.5.1. *Definition of adsorption pseudocapacitance*

The kinetic equation for the net current i passing per cm^2 of S in reaction (3) can be written as [21]:

$$i = Q\frac{d\theta}{dt} \equiv Q\frac{d\theta}{dE}\frac{dE}{dt} = C_p\frac{dE}{dt} = C_p s, \tag{28}$$

where θ is the coverage of deposited metal (M_{ads}) on substrate (S) and Q is the charge required for generation of the monolayer of M_{ads} on substrate (S). C_p, usually called the 'adsorption pseudocapacitance', is to be distinguished from the double-layer capacitance, C_{dl}. Normally $C_p \gg C_{dl}$. $dE/dt = s =$ constant is the so-called sweep rate in a single or repetitive sweeps.

In terms of the kinetic equations, the equilibrium conditions for reaction (3), in the absence of lateral interactions, taking into account the electrosorption valency [21, 40] is

$$k_3(1-\theta)c_{M^{z+}} \exp[\alpha\gamma FE/RT] = k_{-3}\theta \exp[-(1-\alpha)\gamma FE/RT], \tag{29}$$

The electrosorption equilibrium derived from equation (29) is

$$\theta/(1-\theta) = K_3 c_{M^{z+}} \exp(\gamma FE/RT), \tag{30}$$

where $K_3 = k_3/k_{-3}$. In earlier papers it was usually assumed that for surface heterogeneity and/or interaction effects K_3 has the form $K_3^0 \exp(-g\theta)$. It follows from this assumption that there is a linear variation of lateral interaction energy in the monolayer with coverage characterized by a parameter g. However, results measured by temperature programmed desorption in gas/solid experiments [41] and by electrochemical methods [42] show that K_3 is usually neither independent of coverage nor a continuous function of it. K_3 often has a series of discrete values over distinguishable small ranges of θ as the coverage is changed from 0 to 1. This constitutes the phenomenon of 'multiple state' adsorption in monolayers [21].

The adsorption pseudocapacitance ($C_p = Q\,d\theta/dE$) for process (3) can be obtained by differentiation of equation (30) with respect to E. Here Q is the charge required for formation of a monolayer of M_{ads} on substrate (S) but only when $\gamma = z$. Instead of Q, the actual charge $(\gamma/z)Q$ is used in the formation of a monolayer, which has to be substituted into equations when $\gamma < z$ [30, 40].

The adsorption pseudocapacitance is given by [21, 30, 40]:

$$\frac{\gamma}{z}Q\frac{d\theta}{dE} = C_p = Q\frac{\gamma^2 F}{zRT}\theta(1-\theta)$$

$$= Q\frac{\gamma^2 F}{zRT}\frac{K_3 c_{M^{z+}} \exp(\gamma FE/RT)}{[1+K_3 c_{M^{z+}} \exp(\gamma FE/RT)]^2} \tag{31}$$

in terms of θ or E.

Downloaded At: 17:40 21 January 2011

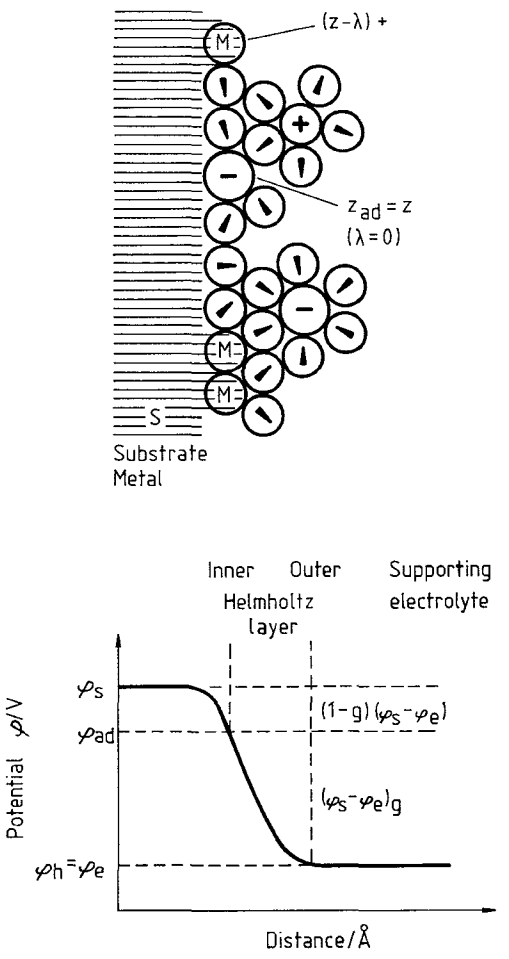

Downloaded At: 17:40 21 January 2011

Figure 1. Schematic double layer model with non-adsorbed ions in the outer Helmholtz layer, adsorbed water molecules and adsorbed ions in the inner layer, when excess supporting electrolyte is used [28].

3.2.5.2. *Capacitance behaviour without lateral interactions*

First the effect of $\gamma < z$ on the form of the C_p against E profile will be evaluated separately by consideration of the anticipated repulsive effects which can arise due to the presence of partially charged species in adsorbed metal layers formed by underpotential deposition.

As can be seen from equation (31), the electrosorption valency enters into the C_p–E relation in two ways. Once as a scaling factor in the pre-exponential factor and then in the exponent. It follows from this that the magnitude of the value of C_p at any potential will be attenuated by the fraction γ^2 and the shape of C_p against E profiles will depend on γ as can be seen from figure 2 [30, 40].

The effect of electrosorption valency in broadening and lowering the C_p against E profiles (figure 2) may be eliminated by an interesting method, which allows the anticipated repulsion to be separately demonstrated.

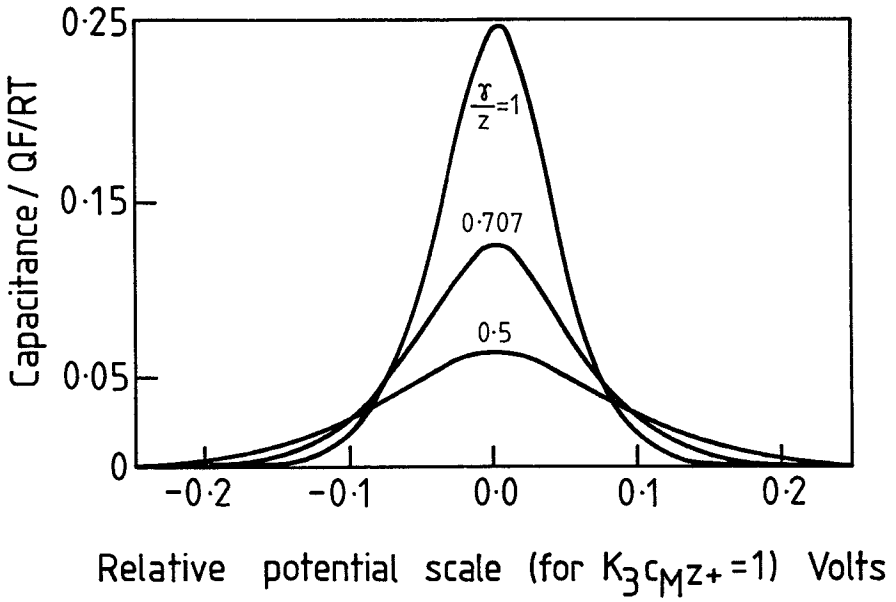

Figure 2. Pseudocapacitance (C) against potential profiles for a one e, single-state UPD process for three values of the electrosorption valency [30].

Downloaded At: 17:40 21 January 2011

From equation (31) it can be seen that the decreasing effect of $\gamma < z$ on C_p against E profile will disappear if a reduced capacitance, $C_p/(\gamma^2/z^2)$ is plotted as $f(E)$. The broadening effect will also disappear if the reduced capacitance is plotted against a scaled potential, $(\gamma/z)E$. The new plot will have the same form as the C_p against E profile for any value of electrosorption valency and will show a Langmuir behaviour [43]. When the lateral interaction effects are taken into account then the increase of the half-widths of $C_p/(\gamma^2/z^2)$ against $(\gamma/z)E$ profiles takes place in a characteristic way as it does in the general case [30, 44].

3.2.5.3. *Lateral interaction effects*

The behaviour of adsorbed species deposited by underpotential deposition is usually reversible and takes place over a characteristic range of potential, very often in multiple states below monolayer coverage, as has been mentioned earlier. This behaviour can be explained by the fact that the adsorbed atoms are deposited in an array or sequential series of arrays rather than as nucleated islands [30]. When partially discharged species are present in the adsorbed layers Coulombic repulsive forces will be expected to operate between adsorbed atoms, thus minimizing the free energy of formation of a 2D lattice array. In this case the adsorption isotherm must contain a term resulting from the long-range 2D free energy of lateral interactions

When the adsorbed metal atoms bear an effective charge $(1-\gamma/z)e$, because $\gamma < z$, the 2D repulsive forces bring about a change of energy of adsorption proportional to $\theta^{3/2}$ if an image surface dipole of $\pm(1-\gamma/z)el$ arises over a charge-separation distance l

[19,40], as has already been mentioned (see section 3.2.3). The lateral interaction energy U is given in the nearest-neighbour approximation [40] as follows:

$$U \approx \frac{n}{2}\frac{\mu^2}{\mathscr{R}^3}\theta^{3/2} = \frac{n}{2}\frac{(1-\gamma/z)^2e^2l^2}{\mathscr{R}^3}\theta^{3/2}, \tag{32}$$

where n is the 2D coordination number of the surface lattice array and $\mathscr{R}$ is the nearest-neighbour distance at $\theta=1$. In this case μ is the surface dipole moment $(1-\gamma/z)el$.

Substituting equation (32) into equation (30) gives

$$\frac{\theta}{1-\theta} = K_3 \exp\left[-\frac{n}{2}\frac{(1-\gamma/z)^2e^2l^2}{\mathscr{R}^3}\frac{\theta^{3/2}}{RT}\right] c_{M^{z+}} \exp\left(\frac{\gamma FE}{RT}\right). \tag{33}$$

Comparing equation (33) with a Frumkin-type isotherm leads to a definition of the (Frumkin) interaction parameter g [40]:

$$g = \frac{n}{2}\frac{\mu^2}{\mathscr{R}^3RT} = \frac{n}{2}\frac{(1-\gamma/z)^2e^2l^2}{\mathscr{R}^3RT} = (1-\gamma/z)^2\frac{r}{RT}. \tag{34}$$

If the partially charged adsorbed metal atoms are regarded simply as adsorbed ions, the interaction potential arises from simple charge repulsion only and would vary as $(n-2)(1-\gamma/z)^2e^2\theta^{1/2}/\mathscr{R}$ [45] and the g parameter is defined by

$$g' = \frac{n}{2}\frac{(1-\gamma/z)^2e^2}{\mathscr{R}RT}. \tag{35}$$

Differentiating equation (33) with respect to E the result is multiplied by $(\gamma/z)Q$ and the required pseudocapacitance will be obtained [40]:

$$C_p = \frac{\gamma}{z}Q\frac{d\theta}{dE} = \frac{\gamma^2QF}{zRT}\frac{\theta(1-\theta)}{1+\frac{3}{2}g\theta^{3/2}(1-\theta)}. \tag{36}$$

In the absence of lateral interaction effects ($g=0$), equation (36) will be simplified and will have the form of equation (31).

In the case of equation (36) an explicit expression cannot be written for C_p as $f(E)$, but numerical evaluation can be made easily, using C_p as $f(\theta)$ from equation (36) together with $\theta=f(E)$ from equation (33) for various values of γ, because the actual magnitude of γ can be determined from separate experiments [40].

If the reduced adsorption capacitance values $(C_p/(\gamma^2/z^2))$ calculated by equation (36) are plotted against scaled potentials $((\gamma/z)E)$, then the lateral interactions in electrodeposited monolayers can be demonstrated for different values of $\gamma<z$. The g factor can be evaluated from the resulting half-widths and interpreted in terms of an adion or surface dipole model of the lateral interactions. The plot of the scaled half-width as $f(g)$ for lateral repulsive interactions between partially charged adsorbed atoms in a random 2D array is almost linear in g for $g>0$ [40].

A more realistic approach to lateral interactions is based on the calculation of electrostatic free energy of interaction (G_e) separately for partial charges and for surface dipoles originating from partial charges and their images [30]. The form of $f(\theta)$ in this case will depend on whether the adsorbed atoms are assumed to interact as simple partial charges, $(1-\gamma/z)e$, or surface dipoles with a surface dipole moment $m=(1-\gamma/z)e\times 2d$ where d is the effective contact distance of adsorbed atoms from the surface of the substrate (S) [30].

Downloaded At: 17:40 21 January 2011

The electrostatic free energy of interaction for partial charges:

$$G_e = \frac{n}{2}\frac{(z-\gamma)^2 e^2}{\varepsilon r}, \tag{37}$$

and for surface dipoles:

$$G_e = \frac{n}{2}\frac{(z-\gamma)^2 e^2 4d^2}{\varepsilon r^3}, \tag{38}$$

where r is the interparticle separation at a coverage θ and ε is the dielectric constant of the interphase.

Taking into consideration that $\mathscr{R}$ is given by $r = \mathscr{R}/\theta^{1/2}$ in relation to θ and r if the substrate surface is a (111), (100) or (110) crystal plane, equations (37) and (38) in terms of θ become

$$G_e = \frac{n}{2}\frac{(z-\gamma)^2 e^2}{\varepsilon \mathscr{R}}\theta^{1/2}. \tag{39}$$

or

$$G_e = \frac{n}{2}\frac{(z-\gamma)^2 e^2 4d^2}{\varepsilon \mathscr{R}^3}\theta^{3/2} \tag{40}$$

respectively [30].

The corresponding adsorption isotherms for the above two cases are

$$\frac{\theta}{1-\theta} = K_3 c_{M^{z+}} \exp\left[-\frac{n}{2}\frac{(z-\gamma)^2 e^2}{2\varepsilon \mathscr{R} kT}\theta^{-1/2}\right]\exp\left(\frac{\gamma FE}{RT}\right), \tag{41}$$

$$\frac{\theta}{1-\theta} = K_3 c_{M^{z+}} \exp\left[-\frac{n}{2}\frac{(z-\gamma)^2 e^2 6d^2}{\varepsilon \mathscr{R}^3 kT}\theta^{1/2}\right]\exp\left(\frac{\gamma FE}{RT}\right). \tag{42}$$

It should be noted that the G_e terms have to be differentiated with respect to the particle number density in order to obtain the chemical potentials of the ad-phase and hence the adsorption isotherms [30].

Earlier papers on image effects indicate that these effects persist even at short distances from metal surfaces but the image potential is modified by a screening factor when d becomes comparable with atomic dimensions. Hence the lateral interactions calculated in terms of repulsion amongst surface dipoles arising from the partial charges and their images provides the preferred basis for the adsorption isotherm of the adsorbed metal atoms deposited by underpotential deposition on foreign metal substrates as it is given by equation (42) rather than equation (41) [30].

In order to obtain the adsorption pseudocapacitance equation (42) has to be differentiated [30]:

$$C_p = \frac{\gamma^2 QF}{zRT}\frac{\theta(1-\theta)}{1+\frac{1}{2}g^*\theta^{1/2}(1-\theta)}, \tag{43}$$

where g^* is the interaction parameter and when $g^* = 0$ then equation (43) will assume the form of equation (31).

Equation (43) is similar to equation (36), thus its application in the evaluation of lateral interactions is also the same. For evaluation of the interaction effects in terms of reduced pseudocapacitance ($C_p/(\gamma^2/z^2)$) calculated by equation (43) at different values

Downloaded At: 17:40 21 January 2011

of g^*, the results must be plotted against scaled potential $((\gamma/z)E)$. Because of the dependence of C_p on θ as well as on $\theta^{1/2}$ terms the shape of the resulting $C_p/(\gamma^2/z^2)$ functions will be asymmetric [30]. The difference between the curves calculated by equations (36) and (43) at different hypothetical g values are the loci of reduced pseudocapacitance maxima. With the use of equation (36) for calculations the loci of the pseudocapacitance maxima are almost independent of the magnitude of g whilst the loci of maxima of the curves obtained by equation (43) are shifted gradually towards a positive range of scaled potentials, with increasing values of g^*.

The half-widths are almost linear in g^* as they are obtained with curves calculated by equation (36).

3.2.5.4. *Conclusions on interaction effects*

The first effects of $\gamma < z$ are the broadening and lowering of the C_p versus E profiles without dependence on some arbitrary parameters (figure 2) and these effects should be manifested in experimental capacitance curves. Experimental C_p against E curves are well resolved into several distinguishable peaks which could not arise if γ were appreciably less than 1 because the broadening and lowering would obscure the distinguishable states of adsorbed metal atoms by overlap [30].

The fact that most experimental results of underpotential deposition show clear resolution into multiple states over a narrow potential range requires that γ be close to z [4, 16, 17, 19, 46]. Another explanation of the experimental observations could be the screening effect by ions of opposite charges and solvent dipoles staying amongst the ad-species in the monolayer [30]. The screening effect, however, must diminish as $\theta \rightarrow 1$ due to exclusion of the screening dipoles or ions from the monolayer, but resolution of multiple states of adsorption in a monolayer is not usually noticeably smaller at high coverages. This indicates that screening effects do not seem to be a major factor in the behaviour of monolayers formed by underpotential deposition [30].

Downloaded At: 17:40 21 January 2011

3.3. *The thin-layer technique in the thermodynamics of UPD*

The twin-electrode thin layer cell [10, 16, 47–49] consists of four electrodes; the working or indicator electrode, the generator electrode and the usual reference and counter electrodes. The generator and indicator electrodes are situated parallel to each other about 50 μm apart and they have independent potential regulation.

The generator electrode must be a reversible electrode for the same metal as that to be deposited at the indicator (working) electrode. The metal ion activity in the cell is given by the potential of the generator electrode according to Nernst's law. The potential of the generator electrode is usually fixed at a certain point, therefore any changes in concentration within the thin layer due to metal ion deposition or dissolution are compensated by the generator.

The advantage of this technique is that the charge and mass fluxes at the indicator electrode can be measured. The charge flux is given by the current density at the indicator electrode, whereas the mass flux to the indicator electrode corresponds to the current density at the generator electrode.

Under the conditions of constant temperature, pressure and electrolyte composition the thermodynamics of the adsorbate on the indicator electrode in the underpotential range $E \geqslant E_N$ is described by q (the charge on the indicator electrode) and Γ (the surface concentration of adsorbed metal on the indicator electrode) as functions of the indicator (E) and generator (E_N) potentials. At constant generator

electrode potential, the chemical potential of the depositing ions in the thin layer of the supporting electrolyte is also constant.

Upon variation of the potential of metal deposition from an initial equilibrium (E_i) at the initial time (t_i) to a new equilibrium (E_f) at the final time (t_f) in the time interval $t_i \leqslant t \leqslant t_f$, the integral of the current at the generator electrode (i_g) will be equal to the mass flux deposited onto the indicator electrode [48,49], and thus,

$$-(zFA)^{-1}\int_{t_i}^{t_f} i_g\,dt = \Gamma(M_{ads_f}, E_f) - \Gamma(M_{ads_i}, E_i), \tag{44}$$

where $\Gamma(M_{ads_i}, E_i)$ is the initial surface concentration and $\Gamma(M_{ads_f}, E_f)$ is the final surface concentration of the metal deposited onto the indicator electrode at constant solution composition and activity of the depositing ions. A is the electrode surface area and the sign is positive for reduction current.

The charge used for metal deposition (or oxidation) can be calculated by the integral of the current at the indicator electrode (i) [48,49]:

$$A^{-1}\int_{t_i}^{t_f} i\,dt = q(E_f, \Gamma_f) - q(E_i, \Gamma_i), \tag{45}$$

where $q(E_i, \Gamma_i)$ is the charge on the electrode at the beginning of polarization and $q(E_f, \Gamma_f)$ is the charge on the electrode at the end of deposition also at constant solution composition and activity of the depositing ions.

At a sufficiently positive potential $E_i > E_{ML}$ the coverage of adsorbed metal on the indicator electrode vanishes

$$\lim_{E\to\infty} \Gamma(M_{ads}, E) = 0, \tag{46}$$

and thus it is possible to determine the absolute values of Γ by the appropriate choice of E_i (where $\Gamma(M_{ads_i}, E_i) = 0$).

When $E_i > E_{ML}$ then the charge on the indicator electrode is at zero coverage and at E_i initial potential is $q(E_i, \Gamma = 0)$.

At a sufficiently negative generator electrode potential (E_g) (where there are no depositing ions in the thin layer) the charge used for double layer charging in the potential interval of underpotential deposition can easily be determined [48,49]:

$$\lim_{E_g\to-\infty} A^{-1}\int_{t_i}^{t_f} i\,dt = q(E_f, \Gamma=0) - q(E_i, \Gamma=0) \equiv A^{-1}\int_{t_i}^{t_f} i_b\,dt, \tag{47}$$

where $q(E_i, \Gamma = 0)$ is the charge on the indicator electrode at the beginning of polarization and $q(E_f, \Gamma = 0)$ is the charge at the end in the supporting electrolyte free of the depositing ions. i_b is the double layer charging current.

Combination of equations (45) and (47) yields the charge (Δq) due to (underpotential) deposition of metal ions onto the indicator electrode [48]

$$A^{-1}\int_{t_i}^{t_f} (i - i_b)\,dt = q(E_f, \Gamma_f) - q(E_f, \Gamma=0) \equiv \Delta q. \tag{48}$$

From equations (44) and (46) the amount of adsorbed material on the indicator electrode can be calculated and from equation (48) the amount of charge used for underpotential deposition may be derived. By partial differentiation of Δq with respect to Γ the electrosorption valency is obtained [48,49].

Downloaded At: 17:40 21 January 2011

The thin layer technique yields thermodynamic data such as adsorption isotherms with high accuracy. Kinetic data cannot be obtained by this method because the system must always be in a quasi-equilibrium state or in the steady state so as to make possible the mathematical treatment of the experimental results [10, 16].

The flow-through thin-layer technique also provides independent q and Γ data at a very high accuracy, thus allowing a direct determination of electrosorption valency [50].

4. The kinetics of underpotential deposition

The formation of adsorbed metal monolayers on foreign metal substrates (S) is a complex process composed of several phenomena. The very first of these is the transport of the depositing ions from the bulk of the (supporting) electrolyte to the substrate surface. The second is the charge transfer (reaction (3)) and then the adsorption of the discharged metal atom on one or more adsorption sites of the substrate metal surface. (There are authors, however, who assume that adsorption precedes charge transfer [51]. In the course of monolayer formation from a multivalent ion this can be the reaction sequence.)

After discharge and adsorption the 2D nucleation and growth phenomena must be taken into consideration in the process of monolayer formation. Before the appearance of bulk deposition the surface diffusion of the deposited metal atoms may play a role in the formation of an UPD layer.

Naturally, any of these phenomena can be the rate-determining step in the course of underpotential deposition. It must be taken into account that the formation of adsorbed metal monolayers on foreign metal substrates is usually carried out in very diluted solutions of the ions to be deposited, so that the mass transport has a profound effect on the kinetics of underpotential deposition. It follows that the most suitable methods for studying the kinetics of underpotential deposition at low solution concentration of the depositing ions involve rotating electrodes [18, 31, 38, 51–53].

Kinetics of underpotential deposition have also been studied at stationary electrodes [10, 16, 17, 26].

In some cases potentiostatic or galvanostatic pulse measurements were used for studying the kinetics of underpotential deposition of metals [10, 26, 54–56].

In the course of underpotential deposition the change of surface concentration of adsorbed species ($\mathrm{d}\Gamma$) is connected with the change of the charge on substrate metal ($\mathrm{d}q_S$), therefore the rate of metal adsorption on foreign metal substrates ($v = \mathrm{d}\Gamma/\mathrm{d}t$) results in an adsorption current density ($i = \mathrm{d}q_S/\mathrm{d}t$) [27]. In the case of use of excess supporting electrolyte and at constant substrate potential the current density of underpotential deposition is [27]

$$i = \left(\frac{\partial q_S}{\partial t}\right)_E = \left(\frac{\partial q_S}{\partial \Gamma}\right)_E \left(\frac{\partial \Gamma}{\partial t}\right)_E = -\gamma F v, \tag{49}$$

taking into consideration equation (8).

With the help of a similar equation the rate of desorption of adsorbed metal atoms can be described [26].

The rate equation depends on the adsorption isotherm chosen to describe the activity of adsorbed metal atoms.

Downloaded At: 17:40 21 January 2011

4.1. *Study of the kinetics of underpotential deposition with rotating electrodes*

As has been mentioned earlier, for the low concentration of the depositing ions ($\leqslant 10^{-4}$ M) in the supporting electrolyte the rotating electrodes are excellent tools to study the kinetics of underpotential deposition. A widely used variety of the rotating electrodes is the rotating ring-disc electrode (RRDE) which is an exceptionally powerful tool for the study of the kinetics of UPD [18, 51, 52, 57]. Construction of RRDE: the disc electrode is made of substrate metal and the ring electrode is preferably made from the same metal deposited on the disc [18, 57].

Before its use in the experiments the RRDE electrode must be pretreated in a strictly reproducible manner to achieve appropriate reproducibility. The pre-treatment is mechanical polishing and then electrochemical stabilization of the surface [18]. This is accomplished by plating the ring with at least ten layers of the metal deposited on the disc electrode [18].

It is very important that in the course of the experiments the depositing ions must undergo convective-diffusion-controlled reduction at the ring electrode. This is achieved by using a sufficiently negative ring potential [18].

The ring electrode response allows quantitative study of the kinetics of underpotential deposition whilst the disc electrode data facilitate the determination of the dynamic electrosorption valency [52]. In the absence of simultaneous adsorption and partial charge transfer the disc current is a measure of the double layer charging component accompanying a shift in the PZC (potential of zero charge) of the substrate metal. The disc current data can be used to evaluate the double layer capacitance as a function of coverage at various potentials of metal deposition and various metal ion concentrations [52].

Downloaded At: 17:40 21 January 2011

4.1.1. *Ring-electrode behaviour*

Two cases of coupling of mass transport with surface phenomena will be considered; fast heterogeneous equilibrium on the disc surface, and slow surface processes.

4.1.1.1. *Diffusion control with coupled heterogeneous equilibrium*

In this case the rate of underpotential deposition is controlled by the diffusion of depositing ions from the bulk of supporting electrolyte and equilibrium is established rapidly between the species adsorbed on the disc electrode and the depositing ions at the disc surface.

The rate of underpotential deposition obtained from the ring response can be calculated from the difference between the instantaneous and fully unshielded ring currents (ΔI_R^t), the ring collection efficiency (N) and the instantaneous coverage (θ_t) of the deposited metal atoms. The rate of underpotential deposition (I_a^t) is given by [52]

$$I_a^t = \frac{\Delta I_R^t}{N} = 0{\cdot}6204 z F A D^{2/3} \nu^{-1/6} \omega^{1/2} (C^b - C_t^s), \tag{50}$$

where C^b and C^s are bulk and surface concentrations respectively and the other symbols have their usual significance.

The instantaneous surface concentration of the depositing ions (C_t^s) can be calculated from equation (16). On the assumption that $\gamma = z$ and the monolayer free

energy decreases linearly with coverage (equation (21)), equation (50) can be converted to

$$I_a^t = 0{\cdot}6204zFAD^{2/3}\nu^{-1/6}\omega^{1/2}\left\{C^b - \left(\frac{\theta_t}{I-\theta_t}\right)\exp\left[f\theta_t + \frac{zF}{RT}(E_{ML}^a - E_{ML}^o)\right]\right\}, \quad (51)$$

where E_{ML}^a is the potential applied in potentiostatic case and θ_t is instantaneous coverage [52].

Instantaneous coverage (θ_t) can be calculated from

$$\theta_t = \frac{1}{\Gamma_s}\int_0^t J_a^t \, dt, \quad (52)$$

where

$$J_a^t = 0{\cdot}6204D^{2/3}\nu^{-1/6}\omega^{1/2}(C^b - C_t^s), \quad (53)$$

and Γ_s is maximum surface concentration at unit coverage [52].

4.1.1.2. *Mass transport coupled to slow surface processes*

When the rate of surface processes are not fast enough compared to convective-diffusion conditions, mixed control will exist. Initially the adsorption rate is high but as coverage increases the activity of the electrode decreases leading to a decrease in the forward rate of underpotential deposition and an increase in stripping (backward) rate. It follows that the potentiostatic transient response of this process is initially mass transport controlled, followed by mixed control and finally results in surface reaction control as the system approaches equilibrium [52].

Adsorption coupled to charge transfer (and/or surface diffusion) will be considered. The absence or presence of control by surface diffusion may be deduced from the magnitude of kinetic parameters [52].

For the UPD process given by equation (3), the flux of depositing ions (M^{z+}) is given by [52]

$$J = k_f' a_{ML}^u C^s - k_b' a_{ML}^c, \quad (54)$$

$$J = D(C^b - C^s)/\delta, \quad (55)$$

where $\delta = 1{\cdot}612D^{1/3}\nu^{1/6}\omega^{-1/2}$, a_{ML}^u is the activity of the uncovered portion of the substrate metal and a_{ML}^c is the activity of the covered portion. $a_{ML}^c/a_{ML}^u = a_{ML}$ is the activity of the deposit.

Due to the coupled charge transfer the rate constants in equation (54) (k_f' and k_b') are potential dependent. Monolayer activities of covered and uncovered portions of the substrate metal can be calculated using the adsorption isotherm obtained from equations (16) and (21). After substituting the results of the calculation of rate constants and monolayer activities in equation (54) the flux of underpotentially deposited species at the disc surface is

$$J = k_f(1-\theta)C^s \exp\left(-\frac{\alpha zF}{RT}E_{ML}^a\right)\exp(-\beta f\theta)$$
$$- k_b\theta\exp\left[(1-\alpha)\frac{zF}{RT}E_{ML}^a\right]\exp[(1-\beta)f\theta], \quad (56)$$

Downloaded At: 17:40 21 January 2011

where β is the adsorption coefficient and the other symbols have their usual significance.

Surface concentration of the depositing species (C^s) under mixed mass transport and potential-dependent adsorption is obtained by the combination of equations (55) and (56). The rate (I_a^t) of underpotential deposition obtained from the ring shielding response is found by eliminating C^s from equation (50) using the result of combination of equations (55) and (56), and thus the UPD rate under mixed control is given by [18, 52]:

$$I_a^t = zFAD\left\{k_f C^b(1-\theta_t)\exp(-\beta f\theta_t)\exp\left(-\frac{\alpha zF}{RT}E_{ML}^a\right)\right.$$
$$\left.-k_b\theta_t\exp\left[(1-\alpha)\frac{zF}{RT}E_{ML}^a\right]\exp[(1-\beta)f\theta_t]\right\}$$
$$\times\left[D+1{\cdot}612D^{1/3}\nu^{1/6}\omega^{-1/2}k_f(1-\theta_t)\exp(-\beta f\theta_t)\exp\left(-\frac{\alpha zF}{RT}E_{ML}^a\right)\right]^{-1}. \quad (57)$$

Several limiting cases of equation (57) corresponding to mass transport control with rapid heterogeneous equilibrium and surface reaction control have been discussed in reference [52].

The rate of underpotential deposition can also be expressed in terms of exchange current density [52]:

$$I_a = I_a^o\left\{\frac{1-\theta_t}{1-\theta_e}\frac{C^s}{C^b}\exp[\beta f(\theta_e-\theta_t)]-\frac{\theta_t}{\theta_e}\exp[-(1-\beta)f(\theta_e-\theta_t)]\right\}, \quad (58)$$

where θ_e is the equilibrium coverage.

Two types of overpotentials may exist for an UPD reaction (equation (16)) under potentiostatic conditions. One is due to the departure of surface concentration from the bulk value (η_c); the other results from the difference in monolayer activity from its final value at equilibrium (η_a). Total overpotential (η_{ads}) is the sum of these ($\eta_{ads}=\eta_c+\eta_a$) [18, 52]:

$$\eta_{ads} = \frac{RT}{\gamma F}\ln\frac{C^s}{C^b}+\frac{RT}{\gamma F}\left[\ln\frac{\theta(1-\theta_e)}{\theta_e(1-\theta)}+f(\theta-\theta_e)\right]. \quad (59)$$

The instantaneous overpotential can be calculated from the ring current data and it is a measure of the extent of departure from equilibrium conditions at any instant during the transient response [52].

4.1.2. *Disc electrode behaviour*

The disc electrode current transient allows the determination of the dynamic electrosorption valency (γ_d), which involves a coupling of charge-separation and charge-transfer components [18, 52]. The dynamic electrosorption valency is defined by [18, 31, 52]:

$$\gamma_d = \frac{1}{F}\left(\frac{\partial q}{\partial\Gamma}\right)_E = \frac{(\partial q/\partial t)_E}{F(\partial\Gamma/\partial t)_E} \quad (60)$$

where $\partial q/\partial t$ is given by the instantaneous disc current transient and $\partial\Gamma/\partial t$ is the instantaneous ring current accompanying the underpotential deposition at the disc.

Downloaded At: 17:40 21 January 2011

γ_d is a measure of the total instantaneous charge that flows during underpotential deposition, due to charge separation and charge leakage processes per mole of deposited metal atoms [18, 52].

The dynamic electrosorption valency at constant applied potential ($\gamma_{d,E}$) [18] is

$$\gamma_{d,E}F = \gamma_{cs,E}F + \gamma_{ct,E}F = \left(\frac{\partial q_S}{\partial \Gamma}\right)_{E_a} + \left(\frac{\partial q_c}{\partial \Gamma}\right)_{E_a}, \tag{61}$$

The charge separation term of dynamic electrosorption valency (γ_{cs}) is a measure of the change in charge on the metal due to two effects:

(*a*) a shift in potential of zero charge caused by work function change accompanying underpotential deposition of metals (γ_{cs}^{ma}), and
(*b*) changes in specific adsorption of anions (γ_{cs}^{aa}) [18].

The charge separation component of dynamic electrosorption valency (γ_{cs}^{ma}) will always result in deviations of dynamic electrosorption valency ($\gamma_{d,E}$) from z (even if anion adsorption does not contribute to the deviation).

The charge-transfer component (γ_{ct}) of dynamic electrosorption valency is also determined by two effects:

(*a*) the Faradic charge-transfer reaction resulting in adsorbed metal monolayer (reaction (3)) (γ_{ct}^{ma}), and
(*b*) chemisorption reactions involving the discharge and adsorption of anions of the solvent, which take place at the same potential where underpotential deposition of metals (γ_{ct}^{aa}) occurs, for instance hydrogen adsorption and oxide formation [18].

Taking into consideration that the charge on the substrate metal (q_S) is a function of the rational potential ($E_R = E_{PZC} - E_a$) and the solution composition (μ) thus,

$$dq_S = \left(\frac{\partial q_S}{\partial E}\right)_\mu dE_{PZC} - \left(\frac{\partial q_S}{\partial E}\right)_\mu dE_a + \left(\frac{\partial q_S}{\partial \mu}\right)_E d\mu. \tag{62}$$

At constant applied potential (E_a) and solution composition (μ)

$$\left(\frac{\partial q_S}{\partial \Gamma}\right)_{E_a,\mu} = \left(\frac{\partial q_S}{\partial E}\right)_\mu \left(\frac{\partial E_{PZC}}{\partial \Gamma}\right)_{E_a} = C_{\mu_s}\left(\frac{\partial E_{PZC}}{\partial \Gamma}\right)_{E_a} = \gamma_{cs,E}^{ma}F, \tag{63}$$

where C_{μ_s} has the dimensions of electrode capacitance at constant coverage [52].

The potentials of zero charge for metals are linearly related to the work function, and the underpotential shift is approximately equal to the difference between the work functions of the substrate and the adsorbate, therefore $\Delta E_{PZC} \approx \Delta U$ [18, 52]. Taking into account equation (22), assuming that $\gamma = z$ and substituting the result into equation (63), we have

$$\gamma_{cs,E}^{ma}F = C_{\mu_s}\frac{RT}{zF\Gamma_s}\left(\frac{\theta}{1-\theta} + f\theta\right). \tag{64}$$

γ_{ct}^{ma} will be equal to z in most cases. The non-Faradic mechanism, when $\gamma_{ct}^{ma} \neq z$, has already been discussed.

If anion adsorption and chemisorption effects are not separable *a priori*, γ_{cs}^{aa} and γ_{ct}^{aa} will also contribute to $\gamma_{d,E}$ [18, 52].

Downloaded At: 17:40 21 January 2011

4.2. *Potentiodynamic study of underpotential deposition using rotating ring-disc electrode technique*

Cyclic voltammetry is the most frequently used method in studying underpotential deposition of metals on foreign metal substrates. The number of UPD peaks on cyclic voltammograms and the width of peaks were considered in interpreting the thermodynamical and adsorption character of underpotential deposition. However, the current at an electrode does not define mass flux to the substrate metal. For this reason, if the cyclic voltammetric method is not combined with a simultaneous method of monitoring the flux of depositing ions at the substrate metal, interpretation of the cyclic voltammetric data becomes ambiguous for two reasons [53].

Firstly, as can be seen from section 4.1.2, underpotential deposition modifies the double layer structure [53].

Secondly, underpotential equilibrium may not be rapidly established and simultaneous chemisorption processes may interfere with UPD. On the other hand, different phenomena, such as diffusion, charge transfer or adsorption, can be the rate-determining step of UPD. The rate laws of these phenomena will also influence the shape of cyclic voltammograms. The different potential dependence of the rate determining steps must be taken into consideration in the analysis of potentiodynamic responses [53].

Downloaded At: 17:40 21 January 2011

4.2.1. *Ring electrode response*

Models including mass transfer, charge transfer and adsorption kinetics will be analysed below.

4.2.1.1. *Potential scan control with rapid heterogeneous equilibrium*

In this case the rate of underpotential deposition (j_a^E) at any instantaneous potential (E) will be controlled by the potential scan rate ($dE/dt = s$)

$$j_a^E = \Gamma_s\left(\frac{d\theta_E}{dt}\right) = \Gamma_s\left(\frac{d\theta_E}{dE}\right)\left(\frac{dE}{dt}\right) = \Gamma_s s\frac{d\theta_E}{dE}, \tag{65}$$

where θ_E is the coverage at potential E.

The changes in solution composition at the interface are assumed to be negligible in this model [53].

The ring current response is given by

$$I_R^s = I_R - zFANj_a^E, \tag{66}$$

where I_R is the fully unshielded ring current and I_R^s is the shielded ring current response.

Calculating $d\theta_E/dE$ from the combination of equations (16) and (21) and substituting the result into equation (66) yields the ring current [53]:

$$I_R^s = I_R - \frac{zFANs}{RT}\frac{\theta_E(1-\theta_E)}{1+f\theta_E(1-\theta_E)}, \tag{67}$$

4.2.1.2. *Mixed control of surface processes and mass transport*

The concentration of depositing metal ions in supporting electrolyte is usually low and so the rate of underpotential deposition can be under mixed control of mass transport and/or surface processes (adsorption and charge transfer). The potentiodynamic ring current is obtained by the same method as described in section 4.1.1.2 [52, 53].

A detailed description of the derivation of the equation of potentiodynamic ring current can be found in references [52] and [53]. Therefore only two limiting cases will be outlined here.

(*a*) Rapid heterogeneous equilibrium with mass transport control.

In this case the potentiodynamic ring current is given by

$$I_R - I_R^s = (NzFAD/\delta)(C^b - C^s), \tag{68}$$

where

$$C^s = \frac{\theta_E}{1-\theta_E} \exp\left[f\theta_E - \frac{zF}{RT}(E_{ML}^o - E_{ML}^i - st)\right], \tag{69}$$

where $E_{ML}^o - E_{ML}^i$ is an overpotential of underpotential deposition at the initial potential E_{ML}^i [53].

Under these conditions, surface concentration (C^s) may be much lower than bulk concentration (C^b). Equilibrium between the electrode surface covered with adsorbed metal atoms and ions at the substrate surface can be rapidly established. This process results in a convective-diffusion controlled flux at the disc electrode. As coverage increases, C^s will also increase, and finally, at $\theta = 1$, C^s will be equal to C^b.

(*b*) Slow heterogeneous equilibrium with negligible concentration polarization.

Under these circumstances the potentiodynamic ring current is given by [53]

$$I_R - I_R^s = NzFA\left\{k_f C^b \exp\left[-\frac{\alpha zF}{RT}(E_{ML}^{a,i} + st)\right](1-\theta_E)\exp(-\beta f\theta_E) - k_b\theta_E \exp\left[(1-\alpha)\frac{zF}{RT}(E_{ML}^{a,i} + st)\right]\exp[(1-\beta)f\theta_E]\right\} \tag{70}$$

where $E_{ML}^{a,i}$ is the initial absolute potential.

The limiting case may be achieved at very positive applied potentials when the charge transfer in reaction (3) is slow with respect to transport processes [53].

4.2.2. *Disc electrode response*

The potentiodynamic disc electrode response yields also the value of dynamic electrosorption valency but at constant solution composition ($\gamma_{d,\mu}$), and this is again composed of charge separation (γ_{cs}) and charge transfer (γ_{ct}) contributions [18, 53]

$$\gamma_{d,\mu}F = \left(\frac{\partial q}{\partial \Gamma}\right)_\mu = \gamma_{cs,\mu}F + \gamma_{ct,\mu}F. \tag{71}$$

Underpotential deposition results in a negative shift in the potential of zero charge. Usually, the potential is also scanned negatively when investigation of UPD takes place by cyclic voltammetry. Because of the shift of PZC, charging current will arise and the direction of this current will be opposite to that due to the potential scan.

From equation (62) at constant solution composition [18]:

$$\gamma_{cs,\mu}F = \left(\frac{\partial q_S}{\partial \Gamma}\right)_\mu = C_{\mu,s}\left(\frac{\partial E_R}{\partial \Gamma}\right)_\mu. \tag{72}$$

Downloaded At: 17:40 21 January 2011

The non-Faradic charge separation current (i_{cs}) will be [18]

$$i_{cs} = \gamma_{cs,\mu} F \frac{d\Gamma}{dt} = C_{\mu,s} \frac{dE_{PZC}}{dt} - C_{\mu,s} \frac{dE_a}{dt}. \tag{73}$$

From equation (73) it follows that there will be no charging current when the scan rate (dE_a/dt) is equal to the rate of shift of potential of zero charge (dE_{PZC}/dt).

The charge-transfer contribution to electrosorption valency is [18, 53]:

$$\gamma_{ct,\mu} F = \gamma^{ma}_{ct,\mu} F + \gamma^{aa}_{ct,\mu} F = \left(\frac{\partial q_{ma}}{\partial \Gamma}\right)_\mu + \left(\frac{\partial q^a}{\partial \Gamma^-}\right)_\mu \left(\frac{\partial \Gamma^-}{\partial \Gamma}\right)_\mu. \tag{74}$$

The $\gamma^{ma}_{ct,}$ contribution to the charge-transfer portion ($\gamma_{ct,\mu}$) of dynamic electrosorption valency is due to the charge transfer (reaction (3)) of underpotential deposition. The simultaneous chemisorption reactions are taken into account by $\gamma^{aa}_{ct,\mu}$. The extent of interaction of the chemisorption processes with underpotential deposition is measured by the coupling factor ($\partial\Gamma^-/\partial\Gamma$). When it is equal to zero, the simultaneous chemisorption reactions do not interact with the underpotential deposition [18, 53].

Downloaded At: 17:40 21 January 2011

4.3. *Conclusions drawn from the study of kinetics with rotating electrodes*

The rate of underpotential deposition can be under mixed control by mass transport and adsorption with coupled charge transfer. The charge transfer coefficient is similar to that observed for bulk deposition. From the dependence of exchange current density and double layer capacitance on applied potential the formation of a randomly adsorbed structure at low coverage and a more ordered structure at higher coverages can be concluded.

The potentiodynamic peak structure not only depends on the thermodynamics of underpotential deposition but also on the kinetics of metal adsorption on foreign metal surfaces.

The formalism proposed for the dynamic electrosorption valency (γ_d) shows that even in the absence of simultaneous chemisorption reactions the value of dynamic electrosorption valency will differ from Faradic reaction valency owing to the shift in the potential of zero charge caused by underpotential deposition.

Experimental details are given in references [18, 52, 53].

4.4. *Kinetics of underpotential deposition with several adsorbed states*

According to the general phenomenological theory of chemisorption reactions [29, 58], a consecutive mechanism can be written in this case in three steps

$$\underset{\text{bulk metal S}}{M_{ads}} \overset{v_1}{\longleftrightarrow} \underset{\text{phase boundary}}{A_1} \overset{v_2}{\longleftrightarrow} \underset{\text{phase boundary}}{A_2} \overset{v_3}{\longleftrightarrow} \underset{\text{supporting electrolyte}}{M^{z+}}. \tag{75}$$

The adsorbed intermediates carry the macroscopic charges, zl_1 in A_1 boundary and $z(l_1+l_2)$ in A_2 boundary, including double layer contributions. v_1, v_2 and v_3 are reaction rates [58].

4.4.1. *Charge and mass balances*

The charge balance of reaction (75) is given by [58]

$$j=\sum_{i=1}^{3}\lambda_i zFv_i+\frac{d\sigma}{dt}, \tag{76}$$

where j is the total current, λ is the partial charge transfer coefficient and σ is the (double layer) charge on the electrode [58].

Variation of (double layer) charge

$$d\sigma=\left(\frac{\partial\sigma}{\partial E}\right)dE+\sum\left(\frac{\partial\sigma}{\partial\Gamma_i}\right)d\Gamma_i+\left(\frac{\partial\sigma}{\partial c_{\mathrm{Mads}}}\right)dc_{\mathrm{Mads}},\quad x=0, \tag{77}$$

where $(\partial\sigma/\partial E)$ is equal to the high-frequency double layer capacity (C_∞).

In the derivation of the combination of equations (76) and (77), the mass balances from equation (76) are [58]

$$d\Gamma_1/dt=v_1-v_2, \tag{78a}$$

$$d\Gamma_2/dt=v_2-v_3. \tag{78b}$$

The l coefficients which contain the double-layer parameters $(\partial\sigma/\partial\Gamma_i)$ are

$$l_1=\lambda_1+(\partial\sigma/\partial\Gamma_1)_E/zF, \tag{79a}$$

$$l_2=\lambda_2+[(\partial\sigma/\partial\Gamma_2)_E-(\partial\sigma/\partial\Gamma_1)_E]/zF, \tag{79b}$$

$$l_3=\lambda_3-(\partial\sigma/\partial\Gamma_2)_E/zF, \tag{79c}$$

and $\sum l_i=1$ [29, 58].

The l coefficient is the same quantity as electrosorption valency [27, 58]. Variation of the double layer structure with underpotential deposition, namely the shift of PZC and co-adsorption phenomena, is taken into consideration in equations (79), and thus the l coefficient is practically the same as dynamic electrosorption valency [58].

Determination of the l coefficient is based on the comparison of mass transport and charge transport in underpotential deposition.

4.4.2. *Charge and mass relations for the potentiostatic step method at rotating ring-disc electrodes or in thin-layer cells*

In this case it is assumed that at the beginning of the potentiostatic experiments, the potential is in a potential range where Γ_1, Γ_2 and $c_{\mathrm{M_{ads}}}$ are practically zero and at $t=0$ the potential is stepped to E in the underpotential range. The disc (working) electrode current (i_{D}) and the ring (generator) electrode current (i_{R}) are derived from equations (76–78);

$$\frac{i_{\mathrm{D}}}{A_{\mathrm{D}}}=j=zFv_1-zF(l_2+l_3)\frac{d\Gamma_1}{dt}-zFl_3\frac{d\Gamma_2}{dt}+\frac{\partial\sigma}{\partial c_{\mathrm{M_{ads}}}}\frac{dc_{\mathrm{M_{ads}}}(x=0)}{dt}, \tag{80}$$

$$\frac{i_{\mathrm{R}}}{zFA_{\mathrm{D}}N}=-v_1+\frac{d\Gamma_1}{dt}+\frac{d\Gamma_2}{dt}, \tag{81}$$

where A_{D} is the area of the disc and the other symbols have their usual significance [58].

Integration of the disc and ring currents yields the charge relation

$$Q_{\mathrm{D}}=\int j\,dt=-zFm_{\mathrm{M_{ads}}}-zF(l_2+l_3)\Gamma_1-zF\,l_3\Gamma_2+\Delta Q \tag{82}$$

Downloaded At: 17:40 21 January 2011

and mass relation

$$Q_R = \int \frac{i_R}{A_D N} dt = zFm_{M_{ads}} + zF(\Gamma_1 + \Gamma_2), \tag{83}$$

where the portion of the completely discharged material (M_{ads}) which is accumulated in the substrate S and diffuses into the bulk of S

$$m_{M_{ads}} = -\int v_1 \, dt \tag{84}$$

and the changing of the double-layer charge caused by metal deposition

$$\Delta Q(c_{M_{ads}}; E) \equiv \int_0^{c_{M_{ads}}} \frac{\partial \sigma}{\partial c_{M_{ads}}} dc_{M_{ads}}, \quad x = 0. \tag{85}$$

It is assumed for the integration that the l_k coefficients are almost independent of adsorption densities [29]. (Equations (80)–(83) can be applied for adsorption as well as desorption experiments. In the latter case the signs of the right-hand sides of equations (81) and (82) are changed [58].)

From equations (77) and (78) the time-dependent current quotient

$$\frac{-i_D N}{i_R} = \frac{l_3 \frac{d\Gamma_2}{dt} + (l_2 + l_3)\frac{d\Gamma_1}{dt} - v_1 - \frac{\partial \sigma}{\partial c_{M_{ads}}} \frac{dc_{M_{ads}}}{dt}}{\frac{d\Gamma_2}{dt} + \frac{d\Gamma_1}{dt} - v_1} \tag{86}$$

and the charge quotient

$$\frac{-Q_D}{Q_R} = \frac{l_3\Gamma_2 + (l_2 + l_3)\Gamma_1 + m_{M_{ads}} + \Delta Q}{\Gamma_2 + \Gamma_1 + m_{M_{ads}}}. \tag{87}$$

If a single intermediate state is formed during underpotential deposition and the amount of $m_{M_{ads}}$ and Q are negligible, the l coefficient is

$$\frac{-Q_D}{Q_R} = \frac{-i_D(t)N}{i_R(t)} = l_3. \tag{88}$$

If the charge/mass quotient (equations (86) and (87)) is found to be independent of potential then it can be concluded that only one term dominates in the denominator and numerator. The corresponding l coefficient results from one step and can be evaluated by equation (88). If experimental Q_D/Q_R values depend on potential then the l coefficients must be determined by a full analysis of the potential dependent adsorption isotherms [29, 58].

4.5. *Study of kinetics of underpotential deposition with pulse methods*

The great advantage of pulse measurements in the investigation of underpotential deposition is the possibility to study the kinetics of metal-ion adsorption [10]. Both galvanostatic and potentiostatic pulse measurements were used to obtain kinetic data.

The kinetics of underpotential deposition of copper on a polycrystalline platinum electrode were determined with galvanostatic pulse measurements of the dependence on copper ion activity, copper coverage and substrate potential [26]. It has been found that the rate-determining process is the charge transfer (reaction (3)) when $\theta < 1$.

Downloaded At: 17:40 21 January 2011

(Similar results were observed in the case of gold substrate [10].) The electrochemical transfer coefficients were also determined and their sum yields electrosorption valency (γ). Based on equation (49), adsorption and desorption current density is given by

$$i_{ads} = -\gamma F k_{ads} c_{M^{z+}} \exp\left(-\frac{\beta_c f\theta}{RT}\right) \exp\left(-\frac{\beta_e(\theta) zFE}{RT}\right), \tag{89}$$

$$i_{des} = \gamma F k_{des} \exp\left(\frac{\alpha_c f\theta}{RT}\right) \exp\left(\frac{\alpha_e(\theta) zFE}{RT}\right), \tag{90}$$

where subscripts c and e denote chemical and electrochemical and the other symbols have their usual significance [26].

Many papers have been devoted to applying galvanostatic or potentiostatic pulse techniques to the problem of deciding between the two different models describing the formation and desorption of adsorbed metal layers. Practically single-crystal surfaces and very often Ag substrates made electrolytically by the Budevski capillary method were used in the experiments [59].

At first the experimental results of underpotential deposition were interpreted in terms of a homogeneous sorption model taking into account the multi-state character of adsorbed monolayers [21]. In this model M^{z+} transfer from the electrolyte to the substrate surface and the surface diffusion of M_{ads} are regarded to be rate-determining steps. In the case of single-crystal substrates surface structure is considered to be composed of distinct homogeneous microregions separated by an array of line discontinuities (grain or subgrain boundaries or monoatomic steps). Metal-ion transfer takes place within the homogeneous regions and at discontinuities. Local differences in the surface concentration of M_{ads} give rise to a 2D mass transport described by a linear surface diffusion model [10, 17, 54, 56, 60].

The adsorption model describes the structure of the adsorbed metal layer at small coverages because the adsorption can proceed by random deposition until approximately half the sites are filled and the adatoms are still quite widely separated. Further increase in coverage necessitates bringing adjacent atoms into very close proximity and this requires the development of nuclei to overcome the electrostatic repulsion between separate adsorbed atoms [61]. This concept involves 2D nucleation and growth steps corresponding to a first-order phase transition process. On the basis of theoretical considerations a discontinuity of the adsorption isotherms at the critical nucleation potential can be expected. The existence of non-monotonous current-time transients under potentiostatic pulse polarization conditions is another evidence of the 2D nucleation and growth model [17, 55, 62–65].

Another important result of these investigations is that in all cases, even for deposition at very high overpotentials, the initiation of bulk deposition by 3D nucleation does not occur until the underpotential monolayer has been formed. The underpotential deposition appears to be an essential precursor to bulk deposition [61]. Ignoring underpotential deposition in theoretical treatments and experimental studies of electrocrystallization on foreign substrates resulted in inadequate models of this phenomenon [17].

5. The study of underpotential deposition by optical methods

The adsorbed metal atoms producing various features seen on linear sweep voltammograms also give rise to the corresponding optical effects [55, 66]. The most common optical methods of investigation of the properties of adsorbed metal atoms on

Downloaded At: 17:40 21 January 2011

metal substrates are ellipsometry, modulation spectroscopy and differential reflectance spectroscopy [16].

In the case of modulation spectroscopy and differential reflectance spectroscopy the relative reflectivity changes $\Delta R/R$ are measured [16, 63, 64, 66–68]. $\Delta R/R$ is defined by

$$\frac{\Delta R}{R} = \frac{R_d - R}{R}, \tag{91}$$

where R_d is the reflectance of the surface covered with adsorbed metal of mean thickness d and R is the reflectance of the substrate free of adsorbed metal.

Differential reflectance spectroscopy combined with cyclic voltammetry is widely used in electrochemistry to study adsorbate properties [16, 55, 66–68]. The $\Delta R/R$ against E curve at constant photon energy resembles the corresponding i–E profile expressing a close relationship between relative reflectivity and covarage. In general, the measurements are carried out at different wavelengths with fixed angles of incidence. In all cases the optical properties of adsorbed metal layers were observed to be different from those of bulk deposits. The measured changes are so large that optical effects from the solution side of the double layer can be neglected. There remain only two effects to be considered, the electroreflectance effect from the metal substrate and the optical contribution from the deposited adsorbed metal layer. Thus the relative change in reflectivity can be written as [55]

$$\frac{\Delta R}{R} = \frac{1}{R}\left(\frac{\partial R}{\partial q}\right)_\theta \Delta q + \frac{1}{R}\left(\frac{\partial R}{\partial \theta}\right)_q \Delta\theta, \tag{92}$$

where q is the surface charge density on the substrate and θ is the coverage of the adsorbed metal. The magnitude of electroreflectance coefficient $(\partial R/\partial q)_\theta$ can be estimated from the slope of $\Delta R/R$–q curve. Generally, this slope is comparatively small and it can be shown that the contribution of electroreflectance to $\Delta R/R$ is negligible. If the deposited atoms are assumed to have a 20% ionic character, then Δq will be about $40\,\mu C\,cm^{-2}$ for a monolayer. In this case $(1/R)(\partial R/\partial q)_\theta \Delta q$ is equal to $+1{\cdot}2\times10^{-3}$ whereas the $\Delta R/E$ values measured under these circumstances are about -2×10^{-2}, therefore neither the sign nor the reflectivity changes are consistent with the effect of electroreflectance [55].

Another important factor which can influence the nature of the reflectance/charge plots is the effective thickness $(\bar{d})$ of the deposited layer because $\Delta R/R$ is proportional to $\bar{d}$ [55]:

$$\bar{d} = \frac{1}{A}\sum_i^n d_i\,\delta A_i, \tag{93}$$

where d_i is the local thickness of the deposit and δA_i is the area of an island of the film on the substrate metal of area A. $\bar{d}$ is proportional to the surface coverage of adsorbed metal atoms and hence to q. This model assumes that the values of optical constants of the investigated system remain independent of the coverage which imply no interactions in the ad-layer.

If the electroreflectance effects are ignored, it can be seen that changes in the gradient of a reflectance–charge plot can be due to either the variations of electrosorption valency or changes in optical properties of the deposited metal layer [55]. From the change in the measured reflectance data for metal layers deposited by underpotential deposition on foreign metal surfaces it can be concluded that metal

Downloaded At: 17:40 21 January 2011

atoms adsorbed at relatively high ΔU are partially discharged whereas the adsorbed metal layers formed at lower ΔU are metal-like monolayers [17].

Later, this method was extended to the investigation of cation adsorption on oxide layers [67, 68].

Details of the fundamentals and experimental techniques of optical reflectance methods have already been extensively discussed in excellent reviews and they are not reviewed here [16, 69].

6. The influence of adsorbed substances on underpotential deposition

It has been recognized long ago that adsorbed substances can have a strong influence on the underpotential deposition of metals [6, 7, 16, 19]. It was observed that underpotential deposition of metals was accompanied by an increase in anion adsorption in spite of great excess of supporting electrolyte [6, 7] and the difference between electrosorption valency and Faraday valency can be attributed to simultaneous adsorption of metal ions and anions [7].

Another example of anion effect on underpotential deposition is demonstrated by cyclic voltammograms measure in the presence of different anions and organic species [16, 19, 70]. It was found that the effect of anions increased with the increase of specific adsorption in the sequence [16, 19, 70]

$$ClO_4^- < F^- < SO_4^{2-} < Cl^- < Br^- < SCN^- < I^-.$$

According to experimental observations, the adsorption of anions and organic substances may cause a decrease in underpotential shift (ΔU) [16, 70], presumably due to reduction in bond strength between the adsorbed metal atom and substrate surface. The complex-forming effect of anions, however, must also be taken into consideration in the explanation of this phenomenon, since the underpotential shift depends also on the activity of the depositing ions (see equation (18)).

Differentiating equation (18) with respect to metal ion activity in the supporting electrolyte yields [70]:

$$\left[\frac{d(\Delta U)}{d \ln a_{M^{z+}}}\right]_{a_{ML}} = \frac{RT}{F}\left(\frac{1}{\gamma} - \frac{1}{z}\right). \tag{94}$$

Using equation (94), we may calculate the electrosorption valency of adsorbed metal atoms in different solutions from the dependence of underpotential shift on metal-ion activity. On the assumption that the activity coefficient of the depositing metal ions in the supporting electrolyte is equal to 1 and with the use of the calculated values of electrosorption valency, the quasi-standard potentials and free-energy differences of underpotential deposition can be calculated [70].

A more detailed discussion of the electrosorption valency in the course of co-adsorption and competitive adsorption is given in reference [36].

The kinetic effects of condensed-phase formation have been discussed in theory for two mechanisms, those of instantaneous and progressive nucleation [71, 72]. The dependence of characteristics of cyclic voltammograms on sweep rate for the two mechanisms of condensed-phase formation provide experimental data to distinguish between the two mechanisms in solutions of different composition [70, 72].

A detailed analysis of the kinetics of underpotential deposition of lead on a silver single crystal in the presence of perchlorate, acetate and citrate has been made. It was found that, in solutions of concentration below 10^{-2} M in the depositing ions the

Downloaded At: 17:40 21 January 2011

process is diffusion controlled, but at higher concentrations nucleation phenomena take over control and the kinetics is affected by anions in line with their adsorbability [70].

During a potentiostatic pulse, the current response in the underpotential region indicates a course obeying the equation derived for underpotential deposition controlled by 2D growth with overlap of growing centres formed by instantaneous nucleation [70]. At the beginning of deposition by the potentiostatic pulse, the rate-determining step of lead deposition is the charge transfer with the formation of a low-density superstructure and later the growth of the compact layer becomes dominant [70].

7. Effect of metal adsorption on hydrogen adsorption

In the case of substrate metals (S) which adsorb hydrogen well, such as Pt, metal adsorption inhibits the hydrogen adsorption because underpotential deposition of metals takes place on the same adsorption sites where hydrogen atoms can adsorb. The number of hydrogen adsorption sites occupied by one adsorbed metal atom (S_r, site requirement) has very often been determined [4, 22, 73, 74, 75]:

$$S_r = \frac{N^S - N^S_{surf}}{N_{M_{ads}}} = \frac{Q^o_H - Q_H}{Q_{M_{ads}}/z}, \tag{95}$$

where N^S is the total number of surface substrate atoms, N^S_{surf} is the number of surface substrate atoms free of adsorbed metal atoms and $N_{M_{ads}}$ is the number of adsorbed metal atoms. These numbers can be obtained experimentally from the quantity of charge required for the oxidation of hydrogen adsorbed on substrate surface free of adsorbed metal atoms (Q^o_H) and on substrate covered with adsorbed metal atoms (Q_H) and that required for the oxidation of adsorbed metal atoms ($Q_{M_{ads}}$) and z is the number of positive charges of the metal ions formed in the course of oxidation of M_{ads}.

The observed values of the hydrogen adsorption sites occupied by one adsorbed metal atom (Sr) on Pt, Ir and Rh are summarized in references [74, 75]. They are very often close to the valency of the given adsorbed metal atom and hardly depend on the kind of substrate metal.

In a few cases, however, there is no agreement about the number of hydrogen adsorption sites covered with one adsorbed metal atom [76]. The greatest discrepancy among the site requirement data can be found in the results of Bi adsorption on Pt. According to the first measurements: $S_r = 2$[22, 73, 77–79]. Later, it was shown that Bi adsorption in $HClO_4$ supporting electrolyte is a more complicated process because some part of the adsorbed Bi does not desorb at anodic polarization. This part was called irreversibly adsorbed Bi and its $S_r = 3$ [22], while under the same circumstances at larger Bi coverages $S_r = 2$ also [73]. (Without regard to these results the phenomenon was re-investigated as cation adsorption on oxide layers [68].)

Some minor discrepancy can be observed among the site requirement data of copper adsorbed on Pt. The results in hydrochloric acid supporting electrolyte are $S_r = 1{\cdot}2$ [80, 81] while in H_2SO_4 solution S_r is only 1 [75]. The discrepancy in the results can be explained by anion adsorption taking place in hydrochloric acid solutions [6].

An unexpected result of investigation of Pd adsorption on Pt is the slight inhibition of hydrogen adsorption on Pt [82]. This observation can also be used for calculation of the number of hydrogen adsorption sites occupied by one adsorbed Pd atom.

Downloaded At: 17:40 21 January 2011

Considering that adsorbed Pd atoms also adsorb hydrogen, site requirement can be calculated by the following relation [82]:

$$S_r = 1 + \frac{2\Delta Q_H}{Q_{Pd}}, \tag{96}$$

where $\Delta Q_H = Q_H^o - Q_H$. Calculated from the experimental data $S_r = 1{\cdot}5$ [82]. The site requirement as a function of coverage was also investigated. The surface requirement decreases with increasing coverage but the significant changes observed for Bi and Au adsorption are lacking here [22, 73, 82, 83].

The number of hydrogen-adsorption sites occupied by one ruthenium atom adsorbed on platinized Pt could also be calculated [84]:

$$S_r = \frac{z}{0{\cdot}85}\left(1 - \frac{Q_H^r}{Q_H^o}\right), \tag{97}$$

where Q_H^r is the charge required for the oxidation of the hydrogen adsorbed on Pt surface covered with adsorbed Ru. The S_r value of a Ru atom adsorbed on Pt is about 1·8 [84].

In the case of UPD studied on single crystal surfaces, two limiting cases of superlattice structure formation must be considered. When $r_{M_{ads}}/r_S \leqslant 1$ (1 : 1 adsorption) and when $r_{M_{ads}}/r_S > 1$ (1 : n multi-site adsorption), where $r_{M_{ads}}$ and r_S denote the radii of the adsorbate and substrate respectively [17]. In the case of 1 : 1 adsorption epitaxial superlattice structures can be formed whereas multi-site adsorption blocking n adsorption sites leads to more complex ordered structures of different density and symmetry [17].

Downloaded At: 17:40 21 January 2011

8. Classification of underpotential deposition of metal ions on foreign metal surfaces

The underpotential deposition of metals on foreign metal substrates is metal deposition in the so-called underpotential range (ΔU). In practice, however, all of the deposited metal oxidized in the underpotential range is called adsorbed metal, that is underpotentially deposited metal regardless of the potential of the deposition.

Naturally, the mechanism and the final result of the reactions of underpotential deposition may depend on the circumstances of the deposition, therefore some classification of the reactions that may result in adsorbed metal atoms on foreign metal surfaces would be advisable. The electrochemical literature is still lacking such a classification but, as has been mentioned in the introduction, the different redox processes resulting in adsorbed metal atoms oxidized in the underpotential range can be classified by the source of electrons consumed in reaction (3).

The different redox processes resulting in adsorbed metal atoms which can be oxidized at a more positive potential than the Nernst potential under the same circumstances will be classified and discussed according to the above concept.

8.1. *Underpotential deposition by electric polarization*

In the electrochemical investigations of underpotential deposition the source of electrons in reaction (3) is a system of electrochemical polarization used in electrochemistry. In practice, polarization of the substrate metal in aqueous solutions can be carried out between the potential of hydrogen and oxygen evolution. In the interpretation of the results, however, the value of the Nernst potential of the depositing

ions has to be taken into consideration to decide the region of underpotential deposition.

If the Nernst potential of the depositing ions is more negative than the potential of the hydrogen electrode in the same supporting electrolyte (for example Pb, Sn, Tl, etc.) then the whole range positive to hydrogen potential is the underpotential range. In the case of investigation of underpotential deposition of noble metals (Cu, Au, Ag, etc.), however, the underpotential range is sometimes quite narrow. Occasionally, it is ignored in the discussion of the results.

8.1.1. *Metal adsorption in the underpotential region*

If the potential of metal deposition (E_d) is more negative than the Nernst potential the depositing ions ($E_d \geqslant E_N$) then metal deposition is actually underpotential deposition, which can be described by reaction (3), although even in this case side reactions may take place. In the most reliable papers dealing with underpotential deposition, the undervoltage–overvoltage transition is rigorously taken into consideration in the interpretation of the results.

8.1.2. *Metal adsorption in the overpotential region*

If the potential of metal deposition (E_d) is more negative than the Nernst potential of the metal ions to be deposited ($E_d < E_N$), underpotential deposition can also be carried out, but in addition to metal adsorption bulk deposition may also take place [4, 85] (figure 3). Formation of a large amount of bulk deposit is avoided by application of depositing ions in low concentration (10^{-3}–10^{-7} M) in the supporting electrolyte. In spite of the low concentration of depositing ions, bulk deposition starts before completion of the first monolayer [4].

The adsorbed metal layer formed at overpotential, under open circuit conditions and in the presence of metal ions, was rearranged which resulted in increased coverage of the adsorbed metal [4, 86]. The rate of rearrangement depended on the concentration of the depositing ions, that is it took place via local cell mechanism [4]. The generally accepted mechanisms for electrocrystallization could be excluded [4]. In the case of less noble metals investigated with the same method, bulk deposition was not observed [87–89].

Similar phenomena have been observed in the case of lead adsorption on silver single-crystal surfaces [90–93]. Structural transformation processes in the course of underpotential deposition of lead occur as a result of incorporation of lead adatoms mainly in the crystal lattice of the terraces on the adsorbent surface at low coverages whilst the rate of structural transformation at high coverages increases with step density [90–93].

The most widely used method in the investigation of underpotential deposition is cyclic voltammetry [16, 19, 21, 46, 68, 78]. If the Nernst potential of the ion investigated is between the limits of potential cycling then underpotential deposition takes place both in the underpotential and overpotential region and thus bulk deposition can be expected [93–97] (figure 4). Depending on sweep rate and concentration of the depositing ions, however, bulk deposition cannot occur [93, 94], but in the interpretation of the results the possibility of bulk deposition must be taken into account since bulk deposition (formation of the second or third layer) on an atomic scale might occur [4, 86].

By application of any electrochemical polarization system in the formation or investigation of adsorbed metal layers the value of the Nernst potential of the ions

Downloaded At: 17:40 21 January 2011

invesgitated must be taken into account in the planning of experiments and in the interpretation of the results.

8.2. *Underpotential deposition by reduction*

Naturally, the source of electrons in reaction (3) is not necessarily a system of electrochemical polarization. It can also be some reducing agent. In this case formation of an adsorbed metal layer on foreign metal substrates, or in other terms, underpotential deposition, may occur without electrochemical polarization, merely by chemical reduction. The processes of spontaneous formation of an adsorbed metal layer and the final results of underpotential deposition by reduction can only be investigated by electrochemical methods.

Underpotential deposition by reduction is an almost entirely ignored field of electrochemistry though its results could have been applied in many fields of chemistry of chemical technology, such as catalyst modification and corrosion.

8.2.1. *Metal adsorption via ionization of pre-adsorbed hydrogen*

In the case of substrate metals which can adsorb hydrogen well, such as Pt and Pd, adsorbed metal layers can be formed on the same substrate via ionization of pre-adsorbed hydrogen. Metal adsorption by this method takes a somewhat different course from that of underpotential deposition by electrochemical polarization. The substrate metal should be saturated with hydrogen first then adsorbing ions are introduced into the supporting electrolyte. Under open circuit conditions, underpotential deposition takes place with simultaneous ionization of the pre-adsorbed hydrogen and increase in the potential of the substrate metal in the positive direction:

$$M^{z+} + zH_{ads} \longrightarrow M_{ads} + zH^{+}. \tag{98}$$

Experimental results have led to the conclusion that underpotential deposition via ionization of pre-adsorbed hydrogen results in an adsorbed metal layer having the same character as obtained by electrochemical methods [73, 81–83].

By application of constant current charging curves the site requirement data can also be determined. The site requirement data for adsorbed metal atoms deposited via ionization of preadsorbed hydrogen were the same as in the case of metal atoms deposited by electrochemical polarization [73, 81–83].

If metal adsorption via ionization of preadsorbed hydrogen results in an adsorbed metal layer of the same character as obtained by electrochemical polarization, the same potential dependence of electrosorption equilibrium must exist (chapter 2.1).

By application of the above concept a new method has been developed for the measurement of electrosorption valency of the metal layers formed via ionization of pre-adsorbed hydrogen [81]. Measurement is based on the assumption that an adsorbed metal layer built up from partially discharged species under appropriate conditions can be reduced to a zero-valent layer.

The charge required for the oxidation of an adsorbed metal layer

$$\mathrm{d}\, q_S = \gamma F\, \mathrm{d}\Gamma, \tag{99}$$

and the charge required for the oxidation of the same adsorbed layer prepared on the same surface after reduction

$$\mathrm{d}\, q_{S_R} = zF\, \mathrm{d}\Gamma. \tag{100}$$

Downloaded At: 17:40 21 January 2011

The ratio of equations (99) and (100) yields electrosorption valency as q_S and q_{S_R} can be determined from charging curves. The experimentally determined γ for copper adsorption was the same as published in the literature [81].

8.2.1.1. *Noble metal adsorption via ionization of pre-adsorbed hydrogen*

As has been mentioned earlier, if underpotential deposition occurs at a potential negative to Nernst potential of the depositing ions then in addition to metal adsorption bulk deposition can also be expected. Experimental results of noble metal adsorption via ionization of pre-adsorbed hydrogen have verified this prediction because underpotential deposition of Cu, Ag, Bi, Au, Pd on platinized Pt substrate took place in two steps [73, 82, 83]. The first step, mostly bulk deposition with simultaneous ionization of adsorbed hydrogen:

$$M^{z+} + ze \longrightarrow M_{bulk}, \tag{101}$$

$$H_{ads} \longrightarrow H^+ + e. \tag{102}$$

When the above step was completed, then under open circuit circumstances and only in the presence of the depositing ions the bulk metal crystals were ionized and the adsorbed metal layer was formed:

$$M_{bulk} \longrightarrow M^{z+} + ze, \tag{103}$$

$$M^{z+} + ze \longrightarrow M_{ads}. \tag{104}$$

Sometimes the mechanism of spontaneous adsorption is even more complex because side reactions may also occur.

This mechanism of rearrangement is the same local cell mechanism as observed at underpotential deposition in the overpotential range [4].

In addition to thermodynamic reasons, kinetic conditions which necessarily lead to bulk deposition will be defined [82]. If the potential of a substrate metal is scanned to a more negative potential than the Nernst potential of a M^{z+}/M system, then the following processes occur [82]:

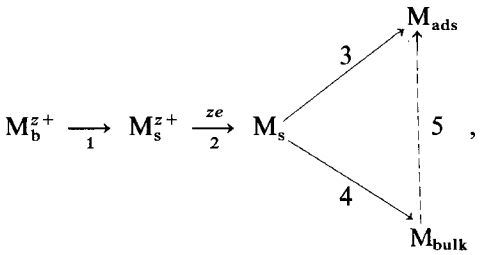

(105)

where process **1** is metal-ion diffusion to the surface, process **2** is charge transfer, process **3** is metal adsorption and process **4** is bulk deposition. With the assumption that the rate-determining step may be either diffusion or adsorption and bulk deposition

$$r_1 = r_3 + r_4. \tag{106}$$

The rate of adsorption is a function of the coverage, consequently, bulk deposition should begin if $r_1 \geqslant r_3$. Because of the slow pore diffusion the effective number of adsorption sites during the first step (reactions (101) and (102)) is very small if

Downloaded At: 17:40 21 January 2011

platinized Pt is used and thus, the ratio of r_3 and r_4 is strongly dependent on surface roughness [4, 82, 98].

When non-equilibrium conditions come to an end (the end of reactions (101) and (102)) the potential of the substrate metal has already been in the underpotential range and in the presence of the depositing ions reactions (103) and (104) started, resulting in the rearrangement (process **5** in reaction (105)) of the system [73, 82, 83].

This mechanism, however, proved to be invalid in Ru adsorption via ionization of hydrogen adsorbed on platinized platinum [84]. The different character of Ru could be explained by the assumption that the rate of charge transfer (process **2** in reaction (105)) is low and for this reason a ruthenium ion has enough time to diffuse into the depth of pores of Pt black, consequently, instead of bulk deposition an adsorbed layer is mainly formed [84].

If underpotential shift (ΔU) is very small (gold adsorption on Pt [83]) then metal adsorption via ionization of preadsorbed hydrogen is a more suitable method than electrochemical procedures for the preparation of adsorbed metal layers.

Downloaded At: 17:40 21 January 2011

8.2.1.2. *Common metal adsorption via ionization of preadsorbed hydrogen*

The Nernst potential of the common metals is more negative than the hydrogen potential and thus bulk deposition cannot be expected during their adsorption via ionization of preadsorbed hydrogen. If side reactions do not occur then

$$M^{z+} + ze \longrightarrow M_{ads}, \tag{107}$$

$$H_{ads} \longrightarrow H^+ + e, \tag{108}$$

is the mechanism of the spontaneously formed adsorbed metal layer while the potential of the substrate metal rises in a positive direction during metal adsorption [99, 100].

Other characteristics of underpotential deposition of common metals by this method is similar to those of noble metals.

8.2.2. *Catalytic disproportionation*

In the course of investigation of tin and rhenium adsorption on platinized Pt, it has been observed that an adsorbed metal monolayer could be formed spontaneously without any external source of electrons used for metal adsorption [100–102] (figure 5). The phenomenon has been called catalytic disproportionation [100, 102]:

$$z_2 M^{z_1+} \rightleftharpoons (z_2 - z_1) M_{ads} + z_1 M^{z_2+}, \tag{109}$$

where the sequence of ionic charges is $z_2 > z_1 > 0$.

Characteristics of adsorbed metal monolayers formed by catalytic disproportionation proved to be similar to those formed by other methods [100].

8.2.2.1. *Thermodynamic reasons of disproportionation*

Naturally, catalytic disproportionation occurs only in the case of ions with several states of oxidation. For example there are M^{z_1+} and M^{z_2+} ions in water solution and they do not disproportionate. It follows that the sequence of their standard redox potentials is

$$E^{\circ}_{M^{z_1+}/M_{bulk}} < E^{\circ}_{M^{z_2+}M_{bulk}} < E^{\circ}_{M^{z_2+}/M^{z_1+}}. \tag{110}$$

In the presence of an adsorbing metal surface, new equilibria appear. The equilibrium constant of catalytic disproportionation (K_d) is given by (111) provided that the activity of M_{ads} is nearly one:

$$K_d = \frac{[M^{z_2+}]^{z_1}}{[M^{z_1+}]^{z_2}}. \tag{111}$$

The thermodynamic condition of equilibrium in a solution in which disproportionation takes place is that the potential of all redox systems are equal to each other. Applying this concept we may calculate the ion activities of equilibrium by equation (16) assuming that ionic charge is equal to electrosorption valency and the ion activities can be substituted for concentrations. Substitution of the results into equation (111) yield

$$\ln K_d = \frac{F}{RT} z_1 z_2 (E^o_{ML_M z_1+/M_{ads}} - E^o_{ML_M z_2+/M_{ads}}). \tag{112}$$

The thermodynamic condition of disproportionation is: $K_d > 1$. This condition is fulfilled only if the following sequence of standard electrosorption potentials is valid [100]:

$$E^o_{ML_M z_1+/M_{ads}} > E^o_{ML_M z_2+/M_{ads}} > E^o_{M z_2+/M z_1+}. \tag{113}$$

If the above conditions are fulfilled, catalytic disproportionation may take place. This is an entirely spontaneous process and results in an adsorbed metal monolayer on a suitable substrate metal surface without any outer source of electrons [100]. The source of electrons in the processes of underpotential deposition in this case is the disproportionation.

8.2.3. *Metal adsorption by polarization with gaseous hydrogen*

Instead of polarization with an electrochemical polarization system a substrate metal can be polarized with gaseous hydrogen if the ionization of hydrogen

$$H_2 \longrightarrow 2H^+ + 2e, \tag{114}$$

can take place on the substrate metal surface. The potential of the substrate metal depends on the partial pressure of hydrogen. For practical reasons, however, the variation of potential of the substrate metal can only be between $-0{\cdot}06$ V and $0{\cdot}1$ V (measured against a hydrogen electrode in the same supporting electrolyte), consequently, the underpotential deposition of common metals can only be carried out by this method because their Nernst potentials are more negative than these potentials. If noble metals are deposited by polarization with hydrogen gas then bulk and adsorbed deposits hardly can be separated.

It is well known that reaction (114) is a catalytic process; this method can therefore be applied if the substrate is one of the metals (Pt, Pd, etc.) used for catalytic hydrogenation.

This method can be used for the modification of metal catalysts with adsorbed metals [103, 104]. The catalysts of catalytic hydrogenation in water solutions are very often modified by addition of different metal ions into the reactor [105, 106].

8.2.4. *The cementation of metals*

If it is true that underpotential deposition is an essential precursor to bulk deposition [61] then the cementation can be interpreted as metal deposition via

Downloaded At: 17:40 21 January 2011

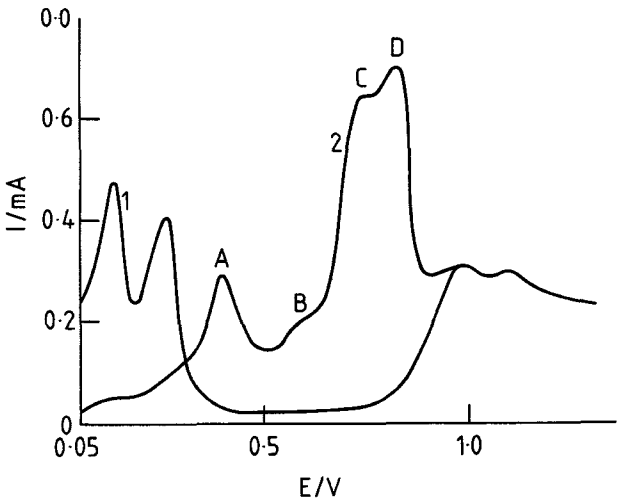

Figure 3. Potential sweep of a Pt electrode in 0·5 M H_2SO_4 solution (1). Potential sweep of the same Pt electrode held at 0·05 V for 14 min in 0·5 M H_2SO_4 containing $CuSO_4$ at the concentration of 3×10^{-6} M (2). Dissolution of bulk deposit (A) and adsorbed species (B, C and D). Sweep rate 5 V s^{-1} (figure 4).

Downloaded At: 17:40 21 January 2011

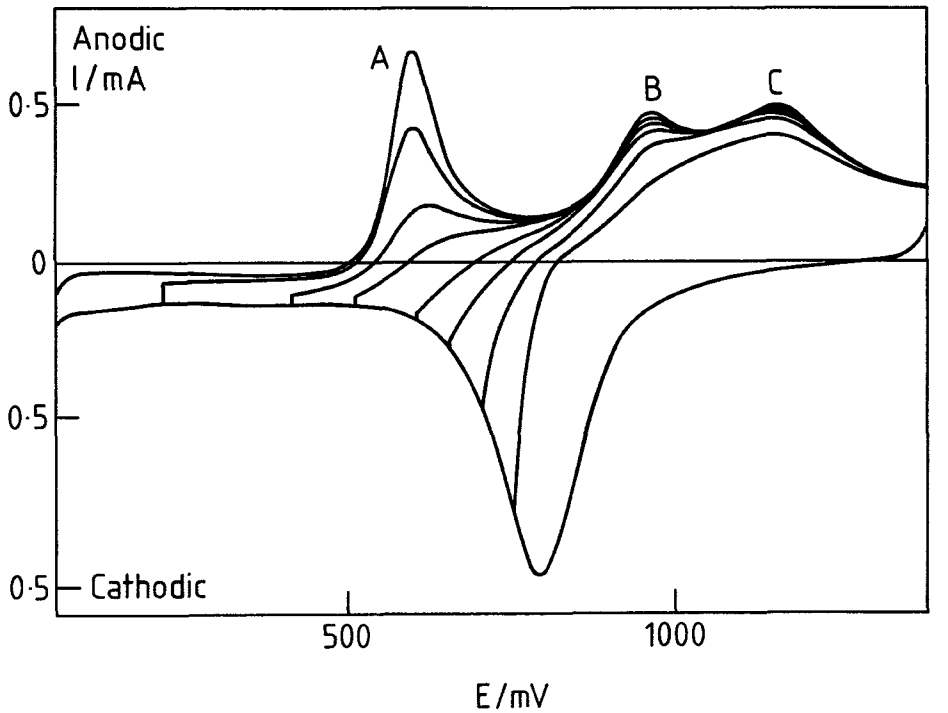

Figure 4. Voltammetry curves of a stationary Pt electrode in the presence of 10^{-4} M Ag^+ in 1 M $HClO_4$ solution. Sweep rate 20 mV s^{-1}. Dissolution of the bulk deposit (A) and adsorbed species (B and C).

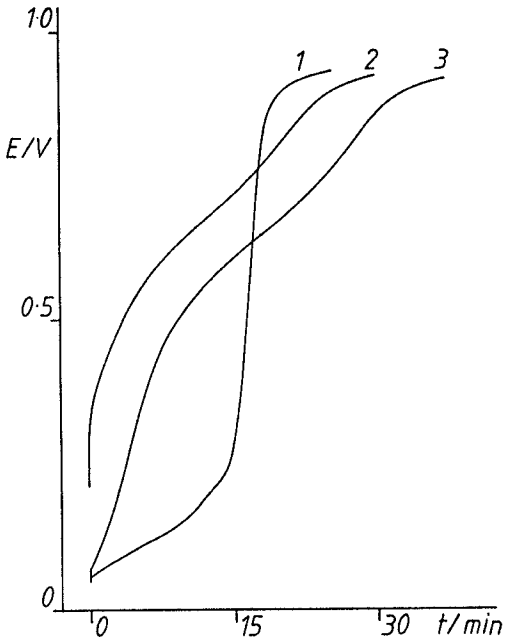

Figure 5. Underpotential deposition of tin by catalytic disproportionation. Charging curve of the platinized Pt electrode in 1 M HCl solution (1). Charging curve in 1 M HCl of the same electrode covered with UPD tin without saturation with hydrogen (2), and as in (2) but after saturation with hydrogen (3). $I = 0{\cdot}25$ mA, concentration of Sn^{2+} is 2×10^{-3} M [100].

ionization of the substrate metal and the very first step of this process must be underpotential deposition. Since the cementation takes place in the overpotential region, therefore bulk deposits appear on the surface after metal adsorption.

If the Nernst potentials of the substrate metal and depositing ions are close to each other then a slow formation of bulk deposit can be expected.

The role of adatoms had been recognized in an early state of investigation of the cementation [107].

8.2.5. *Metal adsorption by polarization with any reducing agent*

Of course, any organic or inorganic reducing agent can be the source of electrons in underpotential deposition of metals on foreign metal surfaces. There are two fields of metal deposition in which adatoms play some role and should be mentioned here. One is contact plating [108] and the other is a process termed as electroless metal deposition [108–110].

9. The physical nature of underpotential deposition

A generally accepted model of the adatom–substrate bond is that the charge transferred from the adatom to the substrate is proportional to the difference in their electronegativities. The chemical bond thus gains a polarity in the electron distribution and this results in an energy gain of the bond [16, 19]. On the other hand, there is a linear correlation between Pauling's electronegativity (x_M) of a metal atom and the work function (Φ) of the same metal [111, 112]. The empirical formula is

$$x_M = 0{\cdot}5\Phi\text{–constant} \tag{115}$$

with a constant of value 0·29 for sp metals and 0·55 for transition metals [112].

Downloaded At: 17:40 21 January 2011

From the fact that the difference in the electronegativities is linearly related to the work functions, the underpotential shift (ΔU) is plotted against the difference in work functions between bulk substrate and bulk deposited metal [16, 19]:

$$\Delta U = \alpha \Delta \Phi, \quad \alpha = 0{\cdot}5\,\mathrm{V\,eV^{-1}}. \tag{116}$$

This empirical correlation shows an astonishingly little scatter when working with polycrystalline substrates (figure 6). The extremely good linear relation between underpotential shift and work function differences suggests that the covalent part of the adatom–substrate bond does not differ appreciably from the bond strength between the adatom and the surface of the same metal [16].

The good linear correlation between monolayer and substrate exists as long as no specific interaction between substrate and adsorbate can be found. The points really scattered in figure 6 are those for systems Ag^+/Au, Hg^{2+}/Au and Au^{3+}/Pt. For silver and mercury extensive alloying and therefore covalency in bonds may be expected [15]. No explanation, however, can be given for the Au^{3+}/Pt system where the underpotential shift is very small [83] or for some pairs which show no underpotential effect [19]. When the underpotential effect is missing the differences in work function are relatively small.

A better approach would be to use the underpotential value for the deposition of the first atom obtained by adding the half-width of the desorption peak to the value for the peak [15]. It has been demonstrated using an energy cycle that for an adsorbed metal ion the difference in bodn strengths for two different substrate metals is given by their work-function difference [15].

Values of underpotential shift for the deposition of the first atoms of metals plotted as a function of difference in work functions for the bulk metals [113] results in a straight line which appears to conform well to the model [15].

It has also been reported that equation (116) seems to hold fairly well for underpotential deposition of various metals on 110 gold surface using $\Delta\Phi$ data of the polycrystalline materials [114]. Since it is believed that the 110-face contributes mostly to a polycrystalline surface this result can be understood.

Evaluation of applicability of equation (116) raises the question as to whether $\Delta\Phi$ has to be considered as an absolute value of work function differences. According to experimental observations the work function of the substrate must be higher than that of the adsorbate metal. This seems to be a necessary condition for monolayer formation [16].

The difference in $\Delta\Phi$ can be considered to be a measure of the ionicity of the adatom–substrate bond, furthermore, there is a definite correlation between Pauling's electronegativity of an atom and the work function of the solid [19]. According to Pauling, the polarity of a chemical bond increases with increasing difference in electronegativities of the atoms involved in the bond [28, 115].

Since γ_{PZC}/z is a measure of bond formation between substrate and adsorbate, plotting absolute difference of the electronegativities, $|\Delta x| = |x_S - x_{M_{ads}}|$ of the substrate (x_S) and of the adsorbate (x_M), against γ_{PZC}/z values for mononuclear ions resulted in a reasonable correlation for cations as well as anions (similar correlations can be obtained for non-aqueous solvents) [28, 116]. When $|\Delta x < 0{\cdot}51$, the γ_{PZC}/z ratio is nearly 1 but decreases with increasing Δx [28].

When γ_{PZC}/z is nearly one the bond formed between substrate and adsorbate is a covalent bond ($\lambda \approx -z$), but at $\gamma_{PZC}/z \ll 1$ a mainly electrostatic adsorption without

Downloaded At: 17:40 21 January 2011

Downloaded At: 17:40 21 January 2011

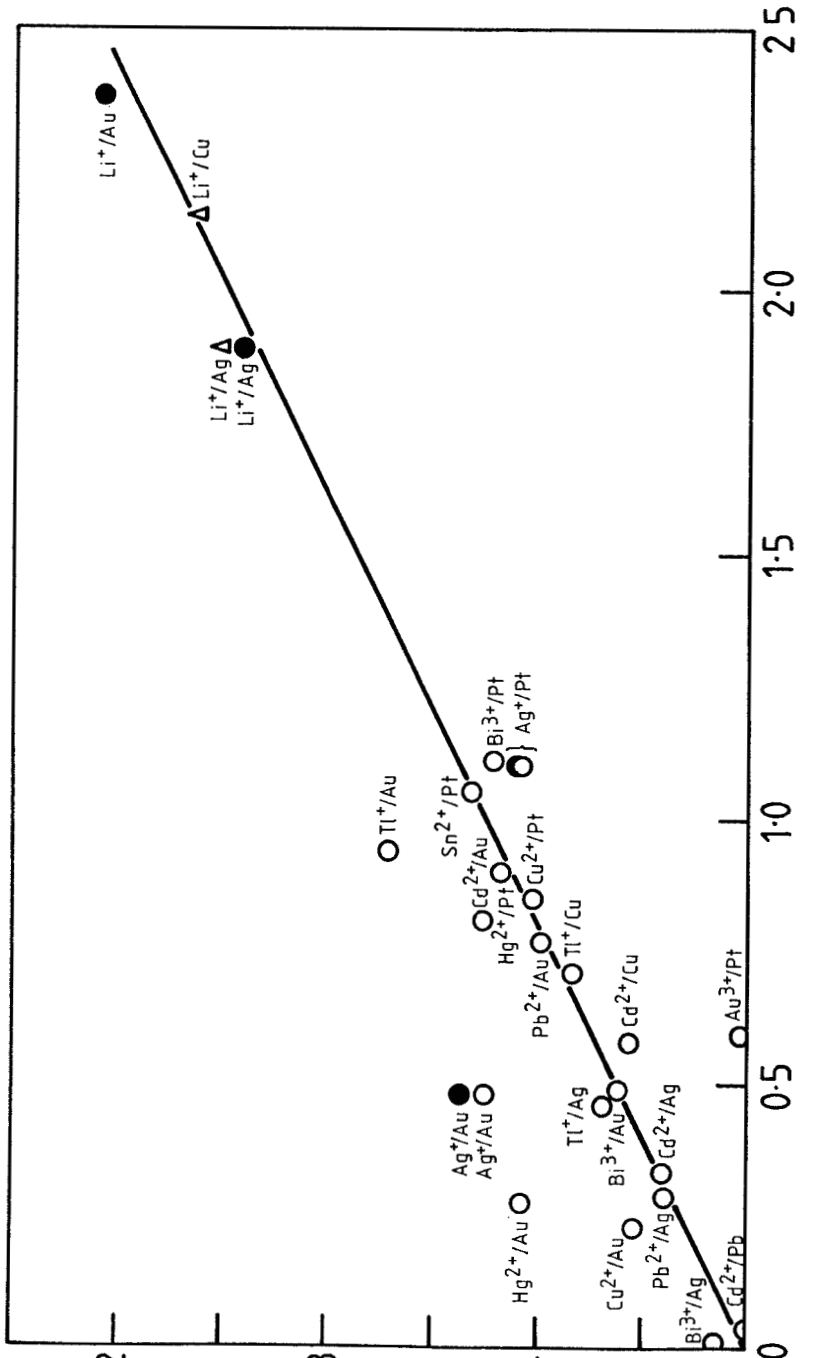

Figure 6. Underpotential shift ΔU between bulk and monolayer stripping peak as a function of $\Delta\Phi$, the difference in work functions of bulk substrate and bulk adsorbed material. (○) aqueous solution, (●) acetonitrile and (△) propylene carbonate [19].

charge transfer ($\lambda \approx 0$) takes place [27, 28]. The formation of polarized bonds with a partial charge transfer is important in the range, $0{\cdot}3 < |\Delta x| < 1{\cdot}0$.

According to Pauling the covalent bond formation and, consequently, the charge transfer can be evaluated from the difference of electronegativities using the following empirical relation [28, 115]:

$$-\lambda/z = \exp[-a(\Delta x)^2]. \tag{117}$$

This formula describes the charge transfer in diatomic molecules in the gas phase, but it will not be valid with the same constant a in aqueous solutions. Because of its large dielectric constant, the water supports the ionization, therefore a higher constant a can be expected for aqueous media [28].

The geometric factor g increases with increasing charge transfer and in the range, $|x| < 0{\cdot}3$, where underpotential deposition generally takes place, the assumption for g is [28]

$$g = g_{\min} - b(\lambda/z), \tag{118}$$

where $b = 0{\cdot}84 = 1 - g_{\min}$, since λ/z is generally negative.

The combination of equation (118) with equations (13) and (117) yields [28]

$$\gamma_{PZC}/z = g_{\min} + 2b\exp[-a(\Delta x)^2] - b\exp[-2a(\Delta x)^2]. \tag{119}$$

This equation describes the correlation between absolute difference of electronegativities and electrosorption valency, fits the experimental data well and can give a rough idea of the real distribution of charge. Of course, differences in the hydration of ions, in bond length, in crystallographic orientation and in the band structure of the substrate may be reasons for deviations of experimental data from the assumed model [28]. On the other hand, the qualitative agreement is reasonable, and this justifies the qualitative application of the model [28].

Downloaded At: 17:40 21 January 2011

Acknowledgments

The author wishes to express his thanks to Professor F. Nagy for stimulating discussions and to Professor F. Márta for his encouragement of this monograph. The financial support of the Hungarian Research Fund (No. OTKA: 1004) is gratefully acknowledged.

References

[1] Hevesy, G. V., 1912, *Phys. Z.*, **13**, 715.
[2] Haissinsky, M., 1933, *J. chim. Phys.*, **30**, 27.
[3] Taylor, A. H., Kirkland, S., and Brummer, S. B., 1971, *Trans. Faraday Soc.*, **67**, 809.
[4] Furuya, N., and Motoo, S., 1976, *J. electroanal. Chem.*, **72**, 165.
[5] Breiter, M. W., 1969, *Trans. Faraday Soc.*, **65**, 2197.
[6] Horányi, G., and Vértes, G., 1973, *J. electroanal. Chem.*, **45**, 295.
[7] Horányi, G., 1974, *J. electroanal. Chem.*, **55**, 45.
[8] Bowles, B. J., 1965, *Electrochim. Acta*, **10**, 717.
[9] Mikuni, F., and Takamura, T., 1970, *Denki Kagaku*, **38**, 113.
[10] Lorenz, W. J., Hermann, H. D., Wüthrich, N., and Hilbert, F., 1974, *J. electrochem. Soc.*, **121**, 1167.
[11] Somorjai, G. A., 1981, *Chemistry in Two Dimensions* (London: Cornell University Press).
[12] Schardt, B. C., Stickney, J. L., Stern, D. A., Wieckowski, A., Zapien, D. C., and Hubbard, A. T., 1987, *Langmuir*, **3**, 239.
[13] Nishimura, K., Machida, K., and Enyo, M., 1988, *J. electroanal. Chem.*, **257**, 21.
[14] Romeo, F. M., Tucceri, R. I., and Posadas, D., 1988, *Surf. Sci.*, **203**, 186.
[15] Trasatti, S., 1975, *Z. phys. Chem. N.F.*, **98**, 75.

[16] KOLB, D. M., 1978, *Advances in Electrochemistry and Electrochemical Engineering*, Vol. 11, edited by H. Gerischer and C. W. Tobias (New York: John Wiley), p. 25.
[17] JÜTTNER, K., and LORENZ, W. J., 1980, *Z. phys. Chem. N.F.*, **122,** 163.
[18] SWATHIRAJAN, S., and BRUCKENSTEIN, S., 1983, *Electrochim. Acta*, **28,** 865.
[19] KOLB, D. M., PRZASNYSKI, M., and GERISCHER, H., 1974, *J. electroanal. Chem.*, **54,** 25.
[20] STUCKI, S., 1977, *J. electroanal. Chem.*, **80,** 375.

[21] CONWAY, B. E., and ANGERSTEIN-KOZLOWSKA, H., 1981, *Accts chem. Res.*, **14,** 49.
[22] SZABÓ, S., and NAGY, F., 1978, J. electroanal. Chem., **88,** 259.
[23] RODES, A., FELIU, J. M., and CLAVILIER, J., 1988, *J. electroanal. Chem.*, **256,** 455.
[24] GOSSNER, K., and MIZERA, E., 1981, *J. electroanal. Chem.*, **125,** 359.
[25] SALVAREZZA, R. C., VASQUEZ MOLL, D. V., GIORDANO, M. C., and ARVIA, A. J., 1986, *J. electroanal. Chem.*, **223,** 301.
[26] SCHULTZE, J. W., 1970, *Ber. Bunsenges. phys. Chem.*, **74,** 705.
[27] SCHULTZE, J. W., and VETTER, K. J., 1973, *J. electroanal. Chem.*, **44,** 63.
[28] SCHULTZE, J. W., and KOPPITZ, 1976, *Electrochim. Acta*, **21,** 327.
[29] LORENZ, W., and SALIE, G., 1977, *J. electroanal. Chem.*, **80,** 1.
[30] CONWAY, B. E., and MARSHALL, S., 1983, *Electrochim. Acta*, **28,** 1003.
[31] ADZIC, R. R., and MINEVSKI, LJ. V., 1987, *Electrochim. Acta*, **32,** 125.
[32] VETTER, K. J., and SCHULTZE, J. W., 1972, *Ber. Bunsenges. phys. Chem.*, **76,** 920.
[33] VETTER, K. J., and SCHULTZE, J. W., 1972, *Ber. Bunsenges. phys. Chem.*, **76,** 927.
[34] VETTER, K. J., and SCHULTZE, J. W., 1974, *J. electroanal. Chem.*, **53,** 67.
[35] FRUMKIN, A. N., DAMASKIN, B., and PETRII, O., 1974, *J. electroanal. Chem.*, **53,** 57.
[36] SCHULTZE, J. W., and VETTER, K. J., 1974, *Electrochim. Acta*, **19,** 913.
[37] FLETCHER, S., 1981, *J. electroanal. Chem.*, **118,** 419.
[38] SWATHIRAJAN, S., MIZOTA, H., and BRUCKENSTEIN, S., 1982, *J. phys. Chem.*, **86,** 2480.
[39] ENGELSMANN, K., LORENZ, W. J., and SCHMIDT, E., 1980, *J. electroanal. Chem.*, **114,** 1.
[40] CONWAY, B. E., and ANGERSTEIN-KOZLOWSKA, H., 1980, *J. electroanal. Chem.*, **113,** 63.
[41] TSUCHIYA, S., AMENOMIYA, Y., and CVETANOVIĆ, R. J., 1970, *J. Catal.*, **19,** 245.
[42] ANGERSTEIN-KOZLOWSKA, H., CONWAY, B. E., and SHARP, W. B. A., 1973, *J. electroanal. Chem.*, **43,** 9.
[43] CONWAY, B. E., and GILEADI, E., 1962, *Trans. Faraday Soc.*, **58,** 2493.
[44] CONWAY, B. E., GILEADI, E., and DZIECIUCH, M., 1963, *Electrochim. Acta*, **8,** 143.
[45] BARRADAS, R. G., and CONWAY, B. E., 1961, *Electrochim. Acta*, **5,** 319.
[46] CHIERCHIE, T., and MAYER, C., 1988, *Electrochim. Acta*, **33,** 341.
[47] SCHMIDT, E., and SIEGENHALER, H., 1969, *Helv. Chim. Acta*, **52,** 2245.
[48] SCHMIDT, E., and WÜTHRICH, N., 1970, *J. electroanal. Chem.*, **28,** 349.
[49] BORT, H., JÜTTNER, K., LORENZ, W. J., and SCHMIDT, E., 1978, *J. electroanal. Chem.*, **90,** 413.
[50] SIEGENTHALER, H., and SCHMIDT, E., 1977, *J. electroanal. Chem.*, **80,** 129.
[51] RIEDHAMMER, T. M., MELNICKI, L. S., and BRUCKENSTEIN, S., 1978, *Z. phys. Chem. N.F.*, **111,** 177.
[52] SWATHIRAJAN, S., and BRUCKENSTEIN, S., 1982, *J. electrochem. Soc.*, **129,** 1202.
[53] SWATHIRAJAN, S., and BRUCKENSTEIN, S., 1983, *J. electroanal. Chem.*, **146,** 137.
[54] HERMANN, H. D., WÜRTHRICH, N., LORENZ, W. J., and SCHMIDT, E., 1976, *J. electroanal. Chem.*, **68,** 273, 289.
[55] BEWICK, A., and THOMAS, B., 1975, *J. electroanal. Chem.*, **65,** 911.
[56] ENGELSMANN, K., LORENZ, W. J., and SCHMIDT, E., 1980, *J. electroanal. Chem.*, **114,** 11.
[57] BRUCKENSTEIN, S., and MILLER, B., 1977, *Accts chem. Res.*, **10,** 54.
[58] SALIE, G., 1988, *J. electroanal. Chem.*, **245,** 1.
[59] BUDEVSKI, E., and BOSTANOV, V., 1964, *Electrochim. Acta*, **9,** 477.
[60] JÜTTNER, K., and SIEGENTHALER, H., 1978, *Electrochim. Acta*, **23,** 971.
[61] BEWICH, A., JOVICEVIC, J., and THOMAS, B., 1977, *Faraday Symp. Chem. Soc.*, **12,** 24.
[62] BEWICK, A., and THOMAS, B., 1976, *J. electroanal. Chem.*, **70,** 239.
[63] BEWICK, A., and THOMAS, B., 1977, *J. electroanal. Chem.*, **84,** 127.
[64] BEWICK, A., and THOMAS, B., 1977, *J. electroanal. Chem.*, **85,** 329.
[65] SCHULTZE, J. W., and DICKERTMANN, D., 1978, *Ber. Bunsenges. phys. Chem.*, **82,** 528.
[66] ADZIC, R., YEAGER, E., and CAHAN, B. D., 1974, *J. electrochem. Soc.*, **121,** 476.
[67] ADZIC, R. R., and MARKOVIC, N. M., 1979, *J. electroanal. Chem.*, **102,** 263.
[68] ADZIC, R. R., and MARKOVIC, N. M., 1985, *Electrochim. Acta*, **30,** 1473.

Downloaded At: 17:40 21 January 2011

[69] McIntyre, J. D. E., 1973, *Advances in Electrochemistry and Electrochemical Engineering*, Vol. 9, edited by R. H. Miller (New York: Wiley-Interscience), p. 61.
[70] Jovicevic, J. N., Jovic, V. D., and Despic, A. R., 1984, *Electrochim. Acta*, **29**, 1625; 1985, **30**, 1455.
[71] Bosco, E., and Rangarajan, S. K., 1981, *J. chem. Soc. Faraday Trans. I*, **77**, 483.
[72] Bosco, E., and Rangarajan, S. K., 1981, *J. electroanal. Chem.*, **129**, 25.
[73] Szabó, S., and Nagy, F., 1976, *J. electroanal. Chem.*, **70**, 357.
[74] Furuya, N., and Motoo, S., 1979, *J. electroanal. Chem.*, **98**, 189.
[75] Furuya, N., and Motoo, S., 1980, *J. electroanal. Chem.*, **107**, 159.
[76] Adzic, R. R., 1984, *Advances in Electrochemistry and Electrochemical Engineering*, Vol. 13, edited by H. Gerischer and C. W. Tobias (New York: Wiley), p. 159.
[77] Bowles, B. J., 1970, *Electrochim. Acta*, **15**, 737.
[78] Cadle, S. H., and Bruckenstein, S., 1972, *Anaiyt. Chem.*, **44**, 1993.
[79] Sazbó, S., and Nagy, F., 1978, *J. electroanal. Chem.*, **87**, 261.
[80] Bowles, B. J., 1970, *Electrochim. Acta*, **15**, 589.
[81] Szabó, S., and Nagy, F., 1977, *J. electroanal. Chem.*, **84**, 93.
[82] Szabó, S., and Nagy, F., 1979, *Israel J. Chem.*, **18**, 162.
[83] Szabó, S., and Nagy, F., 1977, *J. electroanal. Chem.*, **85**, 339.
[84] Szabó, S., Bakos, I., and Nagy, F., 1989, *J. electroanal. Chem.*, **271**, 269.
[85] Scortichini, C. L., and Reilley, C. N., 1983, *J. Catal.*, **79**, 138.
[86] Margheritis, D., Salvarezza, R. C., Giordano, M. C., and Arvia, A. J., 1987, *J. electroanal. Chem.*, **229**, 327.
[87] Furuya, N., and Motoo, S., 1977, *J. electroanal. Chem.*, **78**, 243.
[88] Furuya, N., and Motoo, S., 1979, *J. electroanal. Chem.*, **98**, 195.
[89] Furuya, N., and Motoo, S., 1979, *J. electroanal. Chem.*, **99**, 19.
[90] Vitanov, T., Popov, A., Staikov, G., Budevski, E., Lorenz, W. J., and Schmidt, E., 1986, *Electrochim. Acta*, **31**, 981.
[91] Popov, A., Dimitrov, N., Velev, O., Vitanov, T., Budevski, E., Schmidt, E., and Siegenthaler, H., 1989, *Electrochim. Acta*, **34**, 265.
[92] Popov, A., Dimitrov, N., Kashchiev, D., Vitanov, T., and Budevski, E., 1989, *Electrochim. Acta*, **34**, 269.
[93] Barradas, R. G., Fletcher, S., and Szabó, S., 1978, *Can. J. Chem.*, **56**, 2029.
[94] Clavilier, J., Feliu, J. M., and Aldaz, A., 1988, *J. electroanal. Chem.*, **243**, 419.
[95] Parajon Costa, B., Palotta, C. D., De Tacconi, N. R., and Arvia, A. J., 1983, *J. electroanal. Chem.*, **145**, 189.
[96] Rand, D. A. J., and Woods, R., 1973, *J. electroanal. Chem.*, **44**, 83.
[97] Adzic, R. R., Spasojevic, M. D., and Despic, A. R., 1978, *J. electroanal. Chem.*, **92**, 31.
[98] Sticki, S., 1977, *J. electroanal. Chem.*, **80**, 375.
[99] Szabó, S., and Nagy, F., 1984, *J. electroanal. Chem.*, **160**, 299.
[100] Szabó, S., 1984, *J. electroanal. Chem.*, **172**, 359.
[101] Szabó, S., unpublished result.
[102] Nagy, F., and Szabó, S., 1987, *React. Kinet. Catal. Lett.*, **35**, 133.
[103] Mallát, T., Szabó, S., and Petró, J., 1985, *Acta Chim. Hung.*, **119**, 127.
[104] Mallát, T., Szabó, S., and Petró, J., 1987, *Appl. Catal.*, **29**, 117.
[105] Sokolskii, D. V., 1966, *Catalysts of Liquid Phase Hydrogenation* (Alma-Ata: Nauka) (in Russian).
[106] Sokolskii, D. V., and Zakumbaeva, G. D., 1973, *Adsorption and Catalysis by Metals of VIII Group in Solutions* (Alma-Ata: Nauka) (in Russian).
[107] Despic, A. R., Drazic, D. M., and Sepa, D., 1966, *Electrochim. Acta*, **11**, 507.
[108] Graham, A. K., 1971, *Electroplating Engineering Handbook*, third edition (London: Van Nostrand Reinhold Company).
[109] Flis, J., and Duquette, D. J., 1984, *J. electrochem. Soc.*, **131**, 34.
[110] Flis, J., and Duquette, D. J., 1984, *J. electrochem. Soc.*, **131**, 254.
[111] Gordy, W., and Thomas, W. J. O., 1956, *J. chem. Phys.*, **24**, 439.
[112] Trasatti, S., 1971, *J. electroanal. Chem.*, **33**, 351.
[113] Trasatti, S., 1972, *J. chem. Soc. Faraday I*, **68**, 229.
[114] Schultze, J. W., and Dickertmann, D., 1976, *Surf. Sci.*, **54**, 489.
[115] Pauling, L., 1960, *The Nature of the Chemical Bond*, 3rd edn (Ithaca: Cornell University Press).
[116] Koppitz, F. D., and Schultze, J. W., 1976, *Electrochim. Acta*, **21**, 337.

Downloaded At: 17:40 21 January 2011